




Promoter sequence interaction and structure based multi-targeted (redox regulatory genes) molecular docking analysis of vitamin E and curcumin in T4 induced oxidative stress model using H9C2 cardiac cell line

Pallavi Mishra, Gitanjali Tandon, Manoj Kumar, Biswaranjan Paital, Shasanka Sekhar Swain, Sunil Kumar & Luna Samanta

To cite this article: Pallavi Mishra, Gitanjali Tandon, Manoj Kumar, Biswaranjan Paital, Shasanka Sekhar Swain, Sunil Kumar & Luna Samanta (2021): Promoter sequence interaction and structure based multi-targeted (redox regulatory genes) molecular docking analysis of vitamin E and curcumin in T4 induced oxidative stress model using H9C2 cardiac cell line, Journal of Biomolecular Structure and Dynamics, DOI: [10.1080/07391102.2021.1970624](https://doi.org/10.1080/07391102.2021.1970624)

To link to this article: <https://doi.org/10.1080/07391102.2021.1970624>

 View supplementary material [↗](#)

 Published online: 31 Aug 2021.








 Submit your article to this journal [↗](#)

 View related articles [↗](#)

 View Crossmark data [↗](#)



Promoter sequence interaction and structure based multi-targeted (redox regulatory genes) molecular docking analysis of vitamin E and curcumin in T4 induced oxidative stress model using H9C2 cardiac cell line

Pallavi Mishra^{a*} , Gitanjali Tandon^{b#} , Manoj Kumar^c , Biswaranjan Paital^d ,
Shasanka Sekhar Swain^e , Sunil Kumar^f  and Luna Samanta^a 

^aRedox Biology & Proteomics Laboratory, Center of Excellence in Environment and Public Health, Department of Zoology, Ravenshaw University, Cuttack, Odisha, India; ^bSchool of Biosciences, IMS University Courses Campus, Ghaziabad, Uttar Pradesh, India; ^cDepartment of Biophysics, All India Institute of Medical Sciences, New Delhi, Delhi, India; ^dRedox Regulation Laboratory, Department of Zoology, College of Basic Science and Humanities, Odisha University of Agriculture and Technology, Bhubaneswar, Odisha, India; ^eDivision of Microbiology and NCDs, ICMR-Regional Medical Research Centre Bhubaneswar, Bhubaneswar, Odisha, India; ^fComputer Building, Centre for Agricultural Bioinformatics (CABIN), ICAR-Indian Agricultural Statistics Research Institute (IASRI), New Delhi, Delhi, India

Communicated by Ramaswamy H. Sarma

ABSTRACT

A positive association between oxidative stress and hyper-thyroid conditions is well established. Vitamin E (VIT-E) and curcumin (CRM) are considered as potent antioxidant small molecules. Nuclear factor erythroid 2-related factor 2(NRF-2) is known to bind with antioxidant response element and subsequently activate expression of antioxidant enzymes. However, the activation of NRF-2 depends on removal of its regulator Kelch-like ECH-associated protein 1(NRF-2). In the current study, an attempt is made to demonstrate whether effects of VIT-E and CRM are due to direct interaction with the target proteins (i.e. NRF-2, NRF-2, SOD, catalase and LDH) or by possible interaction with the flanking region of their promoters by *in silico* analysis. Further, these results were corroborated by pretreatment of H9C2 cells (1×10^6 cells per mL of media) with VIT-E (50 μ M) and/or CRM (20 μ M) for 24 h followed by induction of oxidative stress via T4 (100 nm) administration and assaying the active oxygen metabolism. Discriminant function analyses (DFA) indicated that T4 has a definite role in increasing oxidative stress as evidenced by induction of ROS generation, increase in mitochondrial membrane potential and elevated lipid peroxidation (LPx). Pretreatment with the two antioxidants have ameliorative effects more so when given in combination. The decline in biological activities of the principal antioxidant enzymes SOD and CAT with respect to T4 treatment and its restoration in antioxidant pretreated group further validated our *in silico* data.

Abbreviations: AKT: Protein kinase B (PKB); ARE: Antioxidant response elements; AsA: ascorbic acid; CAT: Catalase; CRM: Curcumin; DFA: Discriminant function analysis; GPx: Glutathione peroxidase; GR: Glutathione reductase; GSH: Reduced glutathione; IVR: Intervening region; KEAP-1: Kelch-like ECH-associated protein 1; LDH: Lactate dehydrogenase; LPx: Lipid peroxides; MMP: Mitochondrial membrane potential; mTOR: Mammalian target of rapamycin and FK506-binding protein 12-rapamycin-associated protein 1 (FRAP1); NFkB: Nuclear factor kappa-light-chain-enhancer of activated B cells; NRF-2: Nuclear factor (erythroid-derived 2)-like 2; PDB: Protein data bank; ROS: Reactive oxygen species; SOD: Superoxide dismutase; T₄: thyroxine; TH: Thyroid hormone; VIT-E: Vitamin E

ARTICLE HISTORY

Received 14 March 2021
Accepted 16 August 2021



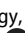

KEYWORDS


Promoter ligand interaction; curcumin; vitamin E; structural binding; NRF-2/KEAP 1 activation

1. Introduction

Thyroid and heart share an intimate and complex functional relationship due to a common embryological origin. Heart is one of the target organs of thyroid hormone (TH) and any dysregulation of TH concentration is associated with development and progression of cardiovascular diseases (Afsar et al., 2017; Bano et al., 2019; Klein, 1990). In hyperthyroidism, TH-induced cardiac hypertrophy is linked to an initial

increase in cardiac function followed by a reduction in cardiac performance signifying the harmful effects of chronic hyperthyroidism (Araujo et al., 2008; da Rosa Araujo et al., 2010; Haglund et al., 2019). Cardiac hypertrophy is a major risk factor for heart failure and associated patient morbidity and mortality (Hunter & Chien, 1999). Hyperthyroidism is associated with increased protein concentration, increased mitochondrial respiration and increased cardiac output leading to increase production of reactive oxygen species (ROS)

CONTACT Biswaranjan Paital  biswaranjanpaital@gmail.com  Redox Regulation Laboratory, Department of Zoology, College of Basic Science and Humanities, Odisha University of Agriculture and Technology, Bhubaneswar, Odisha, 751003, India; Luna Samanta  luna_samanta@rediffmail.com; Isamanta@ravenshawuniversity.ac.in  School of Life Sciences, Ravenshaw University, Cuttack, 753003, Odisha, India

 Supplemental data for this article can be accessed online at <https://doi.org/10.1080/07391102.2021.1970624>

*Department of Zoology, SCS Government College, Puri, Odisha, India

#Centre for Agricultural Bioinformatics, Indian Agricultural Statistics Research Institute, New Delhi, Delhi, India

© 2021 Informa UK Limited, trading as Taylor & Francis Group

resulting in damage to cardiac tissues (Kuzman et al., 2007, Mishra & Samanta, 2012). Augmentation in mitochondrial electron chain activity enhances generation of more ROS such as superoxide anions, hydrogen peroxides, hydroxyl ions (Subudhi et al., 2008, 2009). Overproduction of ROS leads to imbalance of cellular redox status causing oxidative stress in various tissues (Petrulea et al., 2009). The cellular redox homeostasis is maintained by antioxidants that prevent the toxic effects of ROS. The enzymatic antioxidants consist of superoxide dismutase (SOD), catalase (CAT), glutathione peroxidase (GPx) and glutathione reductase (GR) that act in a cascade, while the major non-enzymatic antioxidants are glutathione and ascorbic acid. The SOD dismutates superoxide to hydrogen peroxide that can be neutralized by the either CAT or GPx based on cellular concentration (He et al., 2017).

Nuclear factor erythroid 2-Related Factor 2 (NRF-2) is a conserved leucine zipper protein and a transcription activator which plays a key role in protecting the cell from oxidative stress and inflammation (Sandra et al., 2017). In basal conditions, NRF-2 is bound to its cytoplasmic inhibitory complex formed by Kelch-like ECH-associated protein 1 (NRF-2), and is primarily localized in the cytoplasm (Ahmed et al., 2017). However, under conditions of oxidative stress, specific redox-reactive cysteines of NRF-2 become oxidised, thereby disengaging NRF-2 which translocates to the nucleus to upregulate the expression of genes with Antioxidant Response Elements (ARE) in the promoter region (Nguyen et al., 2009). The upregulated genes include those involved in cellular protection, drug transport, detoxification, and antioxidant defence. NRF-2 protein is expressed in various tissues, such as kidney, muscle, lung, heart, liver, and brain (Mishra et al., 2019; Niture et al., 2014, Li et al., 2019).

In recent years, considerable interest is being shown towards the use of antioxidants as therapeutic agents to target oxidative stress induced pathophysiologic disorders. Vitamin E is a widely studied antioxidant molecule and is useful in mitigating disturbances associated with cardiovascular diseases and cancer (Herberg et al., 1998). CRM is a biologically active phenolic compound derived from the medicinal plant *Curcuma longa* (turmeric). It has been used for thousands of years in Asian countries and traditional Ayurvedic medicine (Gupta et al., 2013). CRM has been shown to have a broad range of antioxidant, antibacterial, antifungal, antiviral, anti-inflammatory, anti-proliferative, and pro-apoptotic properties (Aggarwal & Harikumar, 2009). Recently, we have demonstrated that the administration of vitamin E and CRM resulted in attenuation of the expression of mammalian target for rapamycin (mTOR), restoration of total protein content, biological activity of Ca^{2+} ATPase and oxidative stress indices in hyperthyroid rat heart (Mishra et al., 2019). However, the molecular mechanism(s) involved in the action of VIT-E and CRM and the principal thyroid hormone (thyroxine; T4) in modulation of oxidative stress is poorly understood. Therefore, in the present study, by *in silico* analysis we elucidated the possible interaction of ligands (T4, VIT-E and CRM) with the promoter flanking regions as well as the proteins (SOD, CAT, LDH, KELCH-KEAP1 domain

and KEAP1-NRF 2 domain). The results were validated in rat cardio-myocytic cell lines H9c2 measuring the cellular markers such as Lipid peroxides (LPx), ROS generation, SOD, CAT, Lactate Dehydrogenase (LDH), Mitochondrial Membrane Potential (MMP) as a function of T4, VIT-E and CRM action.

2. Materials and methods

2.1. *In silico* analyses

2.1.1. Molecular docking studies with proteins

The three-dimensional (3D) structures of desired target enzymes, LDH, CAT, SOD, KELCH-KEAP1 domain, and KEAP1-NRF2 domain of human were required as per the objectives of this study by molecular docking. The 3D structure of LDH with Protein Data Bank (PDB) ID: 4ZVV, CAT with PDB ID: 1F4J, SOD with PDB ID: 2JLP, Kelch domain bound to NRF-2 ETGE peptide structure with PDB ID: 5WFV were used and directly retrieved from PDB (<https://www.rcsb.org/>). Similarly, the chemical structures of three ligands, thyroxine, vitamin E, CRM were retrieved from PubChem database (<https://pubchem.ncbi.nlm.nih.gov/>) for binding affinity as well as biological activity against individual target enzymes during docking study. The molecular docking and protein-ligand interaction were visualized with AutoDock 1.4 and BIOVIA Discovery Studio Visualizer v4.5 (BIOVIA DSV) software (Swain et al., 2018).

2.1.2. Molecular docking studies with promoters of the genes

Docking studies have been widely implemented for the study of binding affinity of bio-molecules with ligands. The flanking regions of the promoters were chosen for the study. For our current work, the DNA sequence information was converted to 3D structures using Avogadro software (version 1.2.0) (Hanwell et al., 2012) while the 3D structures of the ligand molecules were directly downloaded from the PubChem Database (Kim et al., 2016). For performing docking, Autodock Vina (1.5.6.) was used. Firstly the pdbqt files for DNA and ligand were created using Graphical User Interface program AutoDock Tools (ADT) as did in our earlier work (Swain et al., 2018). ADT adds polar Hydrogens, solvation parameters, united atom Kollman charges and fragmented volumes to the biomolecules. AutoGrid program was used for preparing the grid map using grid box. The grid size and the grid spacing were set at default. During the docking, both DNA and the ligand molecules were considered as rigid molecules and the results having less than 1.0 Å positional RMSD (Root-Mean-Square Deviation) were clustered together. The obtained complexes were analysed for polar bonds using PyMOL (version 2.3.4) (DeLano, 2002).

2.1.3. Molecular dynamics (MD) simulations

Each of the selected docked complexes was energy minimized to remove any steric clash. It was followed by refinement using molecular dynamics (MD) simulation for 100 ns

to relax the complex with the help of DESMOND (Bowers et al., 2006) simulation program using OPLS 2005 (Jorgensen et al., 1996) force field parameters. Each docked complex was solvated in an orthorhombic box extending to 10 Å from protein atoms in each direction using the TIP3P water model. Solvated complex was neutralized with counter ions followed by energy minimization using steepest descent (SD) algorithm with convergent criteria of 1 kcal/mol/Å. The energy minimized solvated complex was subjected to 100 ns MD simulation at 300 K and 1 atmospheric pressure under Nose-Hoover thermostat and Martyna-Tobias-Klein barostat with periodic boundary condition. Position and velocity of atoms were integrated with the help of RESPA integrator at the time step size of 1 fs. All bonds were constrained with LINCS algorithm. Long range electrostatic forces were calculated by Particle Mesh Ewald (PME) algorithm while cut off scheme was used for short range forces using Verlet scheme for neighbour searching. Other MD run parameters were similar to previous studies (Garg et al., 2020; Kumar et al., 2015). MD trajectory of each complex was analysed for temperature, pressure, volume, energy, root mean squared (r. m. s) deviation, r. m. s fluctuation plot and protein-ligand interactions with respect to time.

2.1.4. Pharmacokinetics prediction

In the drug development module, pharmacokinetics profiles are an essential criterion for selecting active oral drugs. Herein, the pharmacokinetics profiles of CRM, Vit-E, and T4 were predicted using SwissADME (<http://www.swissadme.ch/>) tool, based on individual chemical structure against a considerable training set chemical structure available in the respective database.

2.2. Cell culture

H9C2 cells, a clonal line of cardio-myocytes derived from embryonic rat heart tissue, are extensively used in cardiac research as they are found to possess elements and properties of signalling pathways of adult myocyte (van der Putten et al., 2002). This cell line also provides a useful model system for study of TH uptake and subsequent activity in cardiac cells.

The H9c2 cells were purchased from National Centre for Cell Science (NCCS), Pune, India and cultured in Dulbecco's modified Eagle's medium (DMEM) supplemented with 10% heat inactivated foetal bovine serum, 1% penicillin, 1% streptomycin, and 1% L-glutamine. The cells were cultured and maintained at 37 °C in a humidified atmosphere with 5% CO₂ in an incubator. About 1 × 10⁶ cells per ml of media were incubated for 24 h with CRM (20 μM) or/and vitamin E (50 μM) in a 6-well plate followed by treatment with T4 (100 nM) for 4 h (Li et al., 2000, 2008). Then the cells were washed with PBS (0.01 M, pH 7.4), scrapped and taken out for estimation of intracellular ROS, MMP, membrane damage, protein content and assay of antioxidant enzymes (SOD and CAT).

2.3. Measurement of cell viability (lactate dehydrogenase assay)

Cell viability was measured as a function of LDH released due to membrane damage. The LDH activity was measured in the cell media and also in the cell homogenate (Cabaud & Wroblewski, 1958). This assay is performed to find out the leakage of LDH from the cells into the cell media due to membrane integrity damage. To 2.9 ml tris buffer (0.2 mol/L, pH 7.3), 100 ml of sodium pyruvate (30 mmol/L) and 100 ml of supernatant were added. Immediately the mixture was reacted with 100 ml of NADH (7.5 mmol/L) and change in absorbance of each sample was recorded at an interval of 60 s for 3 min at 340 nm. One unit of LDH has been defined as the amount of protein that will reduce 1.0 mmole of pyruvate to L-lactate per min at pH 7.5 at 37 °C.

2.4. Measurement of intracellular ROS

The formation of intracellular ROS was evaluated using a fluorescent probe, dichlorofluorescein diacetate (DCFH-DA). The non-fluorescent ester penetrates into the cells and is oxidized to the highly fluorescent compound 2', 7'-dichlorofluorescein (DCF) in the presence of ROS. The DCFH-DA dye was dissolved in DMSO and diluted in PBS (0.01 M, pH 7.4) to make a final working solution of 10 μM. Briefly, 1 × 10⁶ cells per ml of media were incubated with 10 μM DCFH-DA in PBS (0.01 M, pH 7.4) at 37 °C for 30 min in dark. Following removal of the DCFH-DA and further washing, fluorescence of the cells from each well was measured using an excitation wavelength of 485 nm and an emission wavelength of 535 nm. Changes in DCFH-DA fluorescence was assayed using FACScan Flow cytometer (Becton-Dickinson Bioscience, San Jose, CA, USA) and data were analysed with CELLQuest Software (Becton-Dickinson Bioscience, San Jose, CA, USA).

2.5. Detection of changes in mitochondrial membrane potential (MMP)

The MMP was monitored using the lipophilic dye JC-1 (5, 5', 6, 6'-tetrachloro-1, 1', 3, 3'-tetraethylbenzimidazolecarbocyanine iodide). Briefly, 1 × 10⁶ cells per mL of media were incubated with 5 mmol/L JC-1 for 30 min at 37 °C. After incubation period, the cells were rinsed with PBS twice, resuspended in PBS (0.01 M, pH 7.4), and instantly assessed for fluorescence using Facsallibur flow Cytometer (Becton-Dickinson Bioscience, San Jose, CA, USA). JC-1 has dual emission depending on the state of mitochondrial membrane potential. JC-1 forms aggregates in cells with a high FL-2 fluorescence indicating a normal MMP. Loss of MMP results in a reduction of FL-2 fluorescence with a counter gain in FL-1 fluorescence as the dye is present in the monomeric state. Thus, 20, 000 gated cells from each sample were analysed on a FL-1 versus FL-2 in a FACScan Flow cytometer (Becton-Dickinson Bioscience, San Jose, CA, USA) and Cell Quest TM software (Becton-Dickinson Bioscience, San Jose, CA, USA).

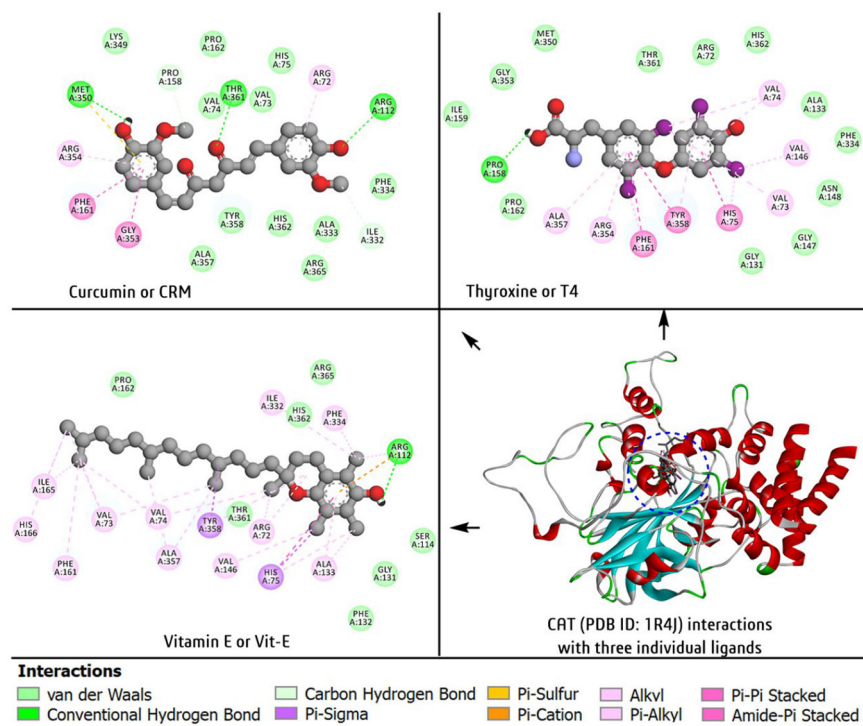


Figure 1. Molecular interaction of ligand-1, 2 and 3 against catalase during docking study. The ligands (levothyroxine as ligand 1, vitamin E as ligand 2 and curcumin as ligand 3) were docked with the modeled human catalase enzyme.

Table 1. Molecular docking score (kcal/mol) of three ligands against five target enzyme/proteins in several combinations.

Enzymes	Ligand-1	Ligand-2	Ligand-3	Ligand-1 + 3	Ligand-2 + 3	Ligand-1 + 2 + 3
LDH	-4.69	-4.77	-4.61	-4.61	-4.61	-4.63
CAT	-4.68	-5.13	-5.21	-5.04	-5.21	-5.34
SOD	-3.37	-4.03	-4.20	-4.21	-4.21	-4.26
NRF2	-4.98	-5.27	-5.26	-4.47	-5.89	-5.59
KEAP1	-4.97	-5.14	-5.29	-4.44	-5.62	-5.17

Ligand-1-thyroxine; ligand-2 -vitamin E, ligand-3 -curcumin, LDH- lactate dehydrogenase, SOD- superoxide dismutase, CAT- catalase, Keap- 1 - Kelch-like ECH-associated protein and NRF-2human nuclear factor erythroid 2-related factor 2.

2.6. Estimation of lipid peroxidation

Lipid peroxidation (LPx) was determined by monitoring formation of thiobarbituric acid reactive substances (TBARS) (Ohkawa et al., 1979). Polyunsaturated lipids are susceptible to free radical-induced oxidation known as LPx. Malondialdehyde (MDA) is the most abundant individual aldehyde by-product of LPx and usually determined based on its reaction with thiobarbituric acid (TBA) in an acidic medium, forming a compound with absorbance maxima at 532nm. For endogenous LPx, 50 μ L of sample (crude/PMF) containing 50-100 μ g of protein was treated with 950 μ L of thiobarbituric acid (TBA) reagent in an acidic medium (20% v/v in acetic acid, pH 3.5) at 95 $^{\circ}$ C for 1 h in presence of butylated hydroxyl toluene to prevent any further ROS damage during incubation followed by centrifugation at 1000 x g for 10min. The absorbance of the supernatant thus formed was taken at 532nm in an UV-VIS spectrophotometer (Cary 100, Varian, USA). The concentration of the resulting TBARS in the supernatant was calculated from its extinction coefficient of malondialdehyde

$1.56 \times 10^5 \text{ M}^{-1} \text{ cm}^{-1}$ and expressed as nmol TBARS formed/mg protein.

2.7. Estimation of antioxidant enzyme activity

For the estimation of antioxidant enzymes in different treated H9c2 cells, 400 μ L of the 12,000 x g supernatant of the cellular homogenate was taken and passed it through a column of Sephadex-G25 to separate the protein fraction from interference of other non-enzymatic small antioxidant molecules (e.g. ascorbic acid, glutathione etc.). The elute thus collected was taken for the assay of SOD activity by a method as described previously based on the scavenging of superoxide released from photo-oxidation of riboflavin and its subsequent conversion to nitrite by hydroxylamine hydrochloride measured by Greiss reagent (Das et al., 2000). Results were expressed as units/mg protein where one unit of enzyme activity was defined as the amount of enzyme capable of inhibiting 50% of nitrite formation under the assay conditions.

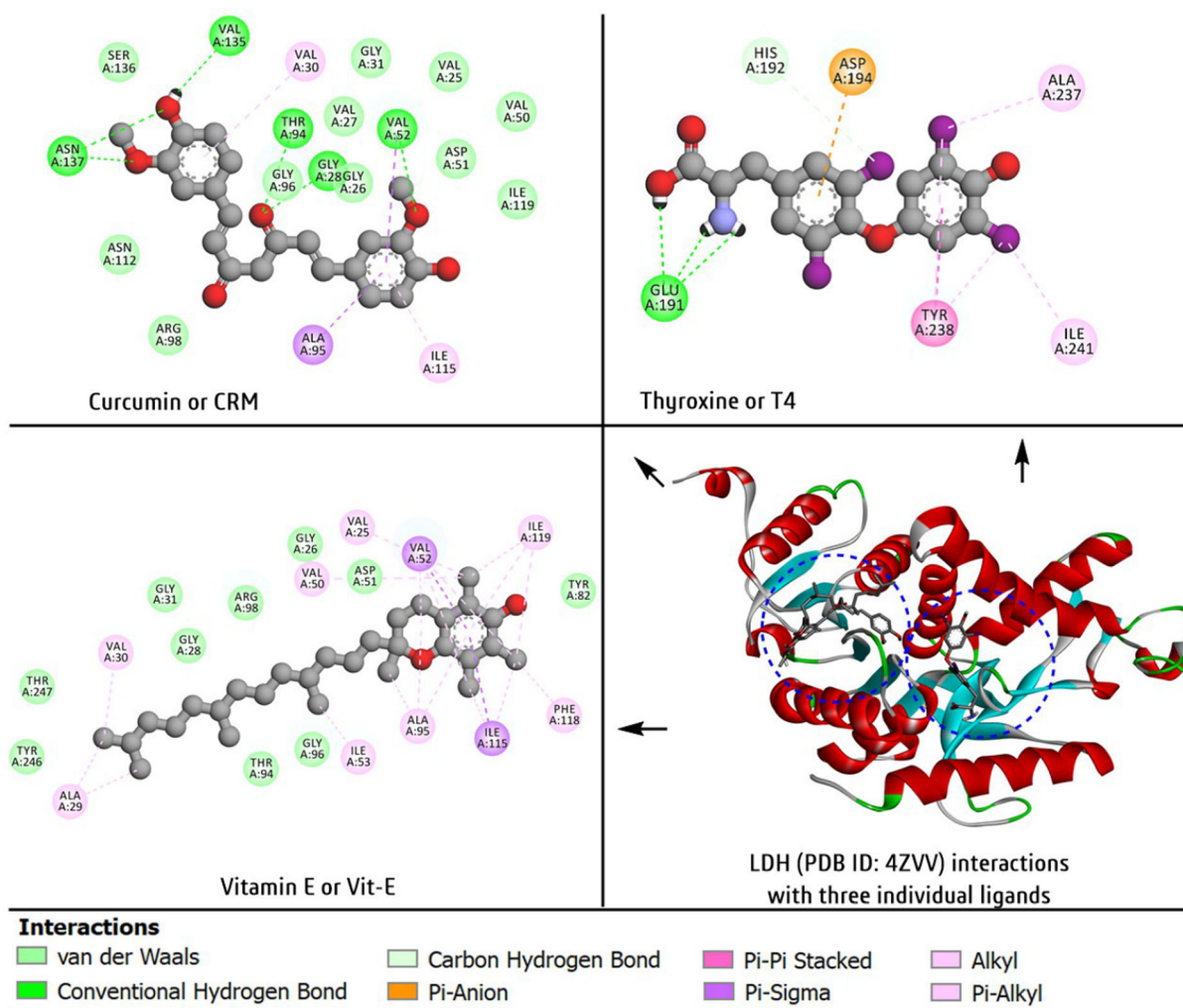


Figure 2. Molecular interaction of ligand-1, 2 and 3 against LDH during docking study.

The ligands (levothyroxine as ligand 1, vitamin E as ligand 2 and curcumin as ligand 3) were docked with the modeled human lactate dehydrogenase (LDH) enzyme.

The CAT activity was assayed according to previously described protocol following the decrease in the absorbance of H_2O_2 at 240 nm after treating the suitably diluted 12,000 x g supernatant of the cellular homogenate with 17 M ethanol to inhibit complex-II formation. Enzyme activity was calculated taking $43.6 \text{ M}^{-1} \text{ cm}^{-1}$ as molar extinction coefficient of H_2O_2 and expressed as μ Katal/mg protein (1 Katal = 1 mol/s) [Cohen et al., 1970; Aebi, 1974]. The protein content was estimated with the help of Bradford reagent, using bovine serum albumin (BSA) as standard at 595 nm (Bradford, 1976).

2.8. Statistics

Each set of data were tested for homogeneity of variance (Levene test) and normality (Lilliefors test). Means were compared and analysed by ANOVA followed by Duncan's new multiple range test for normally distributed data. Differences among the means were considered significant at $p < 0.05$ level. Discriminant Function Analysis (DFA) was performed to evaluate the contribution of the variables of oxidative stress

physiology on differentiation of the studied groups (Paital & Chainy, 2012, 2014).

3. Results

3.1. In silico analysis

In silico analyses indicate that both the protein and promoter regions of the studied enzymes such as SOD, CAT, LDH, KELCH-KEAP1 domain and KEAP1-NRF-2 domain have definite interaction with the ligands, i.e. T4, VIT-E and CRM. The results are presented in the respective sections.

3.1.1. Protein docking

Associated water molecules, ligand, and ions were removed from retrieved targeted five 3D structures for docking study (supplementary Figure 1). Tools of bioinformatics including the docking studies have revolutionized the approach for early drug discovery module by overcoming the traditional hit-and-trail methods (Swain et al., 2015). In the present study, in several cases, synergistic

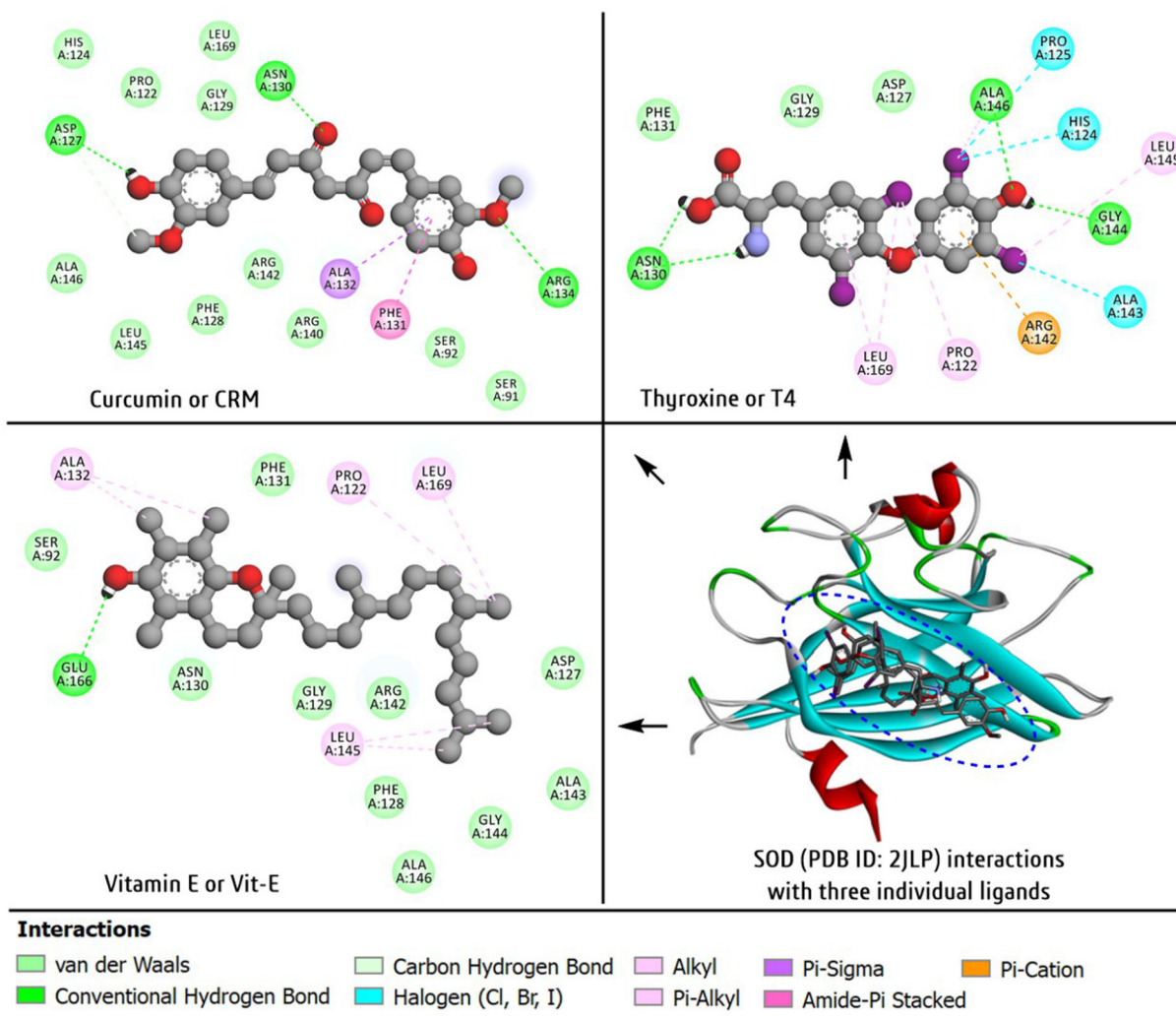


Figure 3. Molecular interaction of ligand-1, 2 and 3 against SOD during docking study. The ligands (levothyroxine as ligand 1, vitamin E as ligand 2 and curcumin as ligand 3) were docked with the modeled human superoxide dismutase (SOD) 1 enzyme.

events showed a comparatively strong binding relationship than that for individual ligand interaction (Table 1). The docking score of each ligand was increased from -4.68 to -5.34 with synergistic docking approach against CAT enzyme (Figure 1); while individual synergistic docking score was slightly decreased against LDH (Figure 2). The docking scores for the studied proteins such as SOD (Figure 3), NRF-2 (Figure 4) and NRF-2 (Figure 5) with T₄ and the nutraceuticals (VIT-E and CRM) were quite prominent (Table 1). Notably, the docking scores with both VIT-E and CRM were significant. Similar results were also observed for all other studied proteins with T₄, VIT-E and CRM taken together with docking scores of -4.63 , -5.34 , -4.26 , -5.59 and -5.17 for LDH, CAT, SOD, KELCH-KEAP1 domain and KEAP1-NRF 2 domain, respectively (Table 1).

3.1.2. Gene promoter docking

Both the flanking regions 5' and 3' end of the DNA sequences of all enzymes were used for studying the interaction

with T₄, VIT-E and CRM. The results are presented systematically in Table 2 and Figures 6–8. Except for the interaction of VIT-E with the flanking regions of SOD2 and NRF-2, the rest of the mammalian promoter sites of CAT, LDH and NRF-2 had quite good numbers of polar bonds with the studied ligands i.e. T₄, VIT-E and CRM. Although there was no polar bonds found for the interaction of VIT-E with the flanking region of the promoters of the studied proteins, the docking scores between the flanking regions of all the proteins and ligands were notably high (Table 2).

When all the three ligands T₄, VIT-E and CRM were docked with SOD1 i.e. CuZn SOD, CRM showed maximum interaction with four polar bonds and -8.4 Kcal/mol binding affinity. Moreover, it was observed that C=O group of the CRM was the most active group with highest number of interactions (Figure 6). On the other hand, T₄ was the most interactive ligand with binding affinity of -6.8 kcal/mol with SOD2 and VIT-E the least interacting partner. When checked for the most active group, C=O group has been the most active group participating in the interaction (Figure 6). Similarly, the 5' region of CAT, T4 had 7 polar bonds showing highest

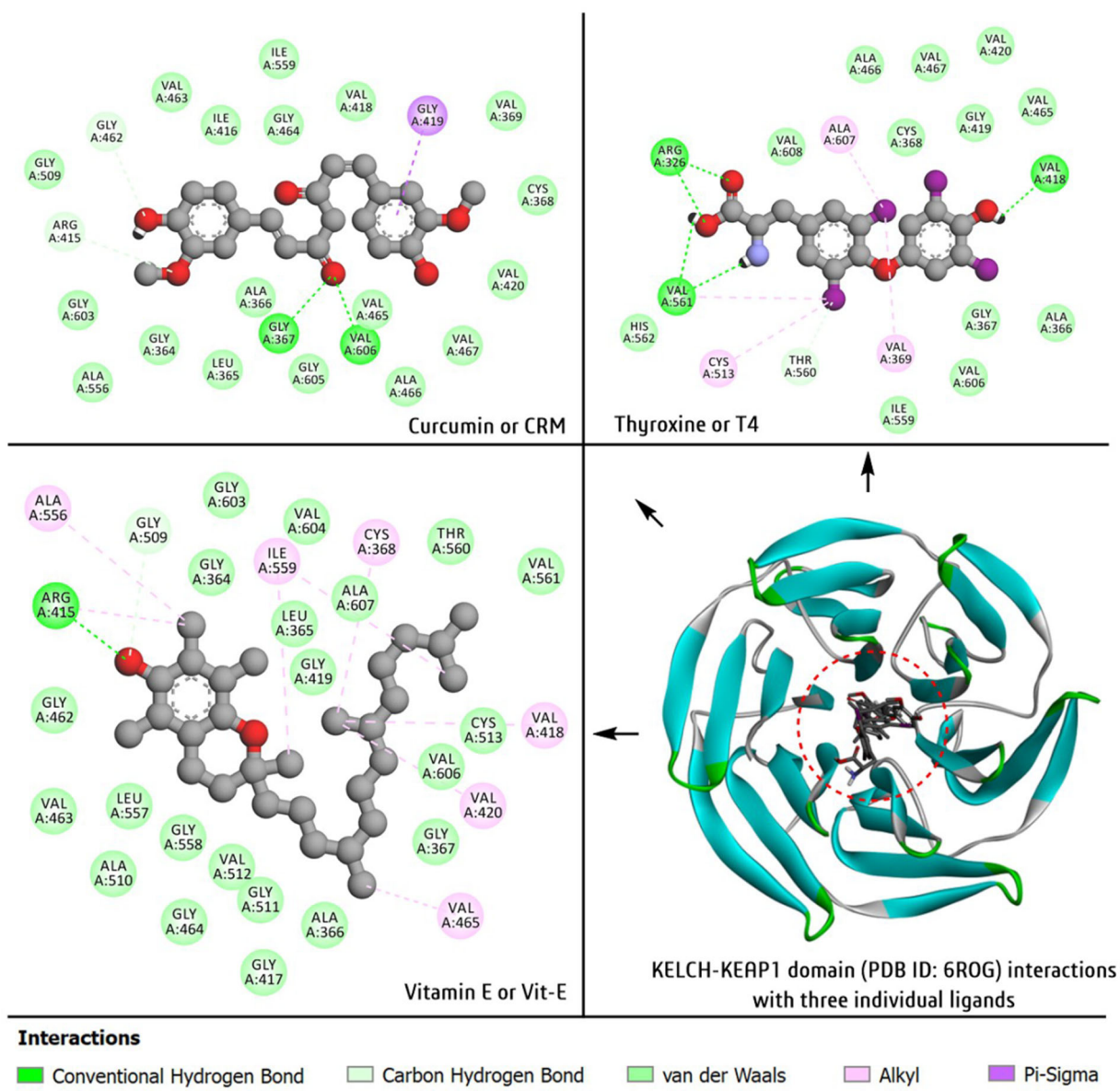


Figure 4. Molecular interaction of ligand-1, 2 and 3 against NRF-2 during docking study.

The ligands (levothyroxine as ligand 1, vitamin E as ligand 2 and curcumin as ligand 3) were docked with the modeled human Kelch-like ECH-associated protein (Keap) 1 protein.

binding ability and involved both C=O and OH groups for stabilization of the interactions (Figure 7). CRM was the most effective ligand for interaction with LDH promoter with formation of 4 polar bonds was having -8.4 kcal/mol binding affinity. Here again, C=O group was found to be the most active group (Figure 7).

When interactions of Keap 1 with T₄, VIT-E and CRM were studied, it was revealed that 3' end of the NRF-2 has been the most interactive partner (as it formed 6 polar bonds) having binding affinity of -6.7 kcal/mol. In this case, both C=O and OH groups were participating in docking (Figure 8). While studying the interaction of NRF-2 with the ligands, it was found that T₄ has been the maximum docked ligand (4 polar bonds) with -6.7 kcal/mol binding affinity while VIT-E did not show any interaction. In this case OH group of the ligand was the most active group binding with many base pairs (Figure 8).

3.1.3. Molecular dynamics (MD) simulations

Analysis of temperature, pressure, volume and energy plot clearly shows that simulation system was stable during simulation. The r. m. s deviation and r. m. s fluctuation plot of protein as well as ligand was analysed to see the dynamic behaviour of protein and especially ligand with respect to time. The r. m. s deviation plot of each complex clearly indicates that both protein and ligand was stabilized between first 40-60 ns of simulation. The r. m. s deviation plot of KEAP1-VIT-E complex shows that protein and ligand both converges around 45 ns while KEAP1-CRM complex converges around 50 ns (Figure 9a and c). Similarly, r. m. s fluctuation plot shows that only variable part of protein (large loop region) and terminal atoms of ligand was fluctuating while rest of the complex were within the thermal vibration range (Supplementary Figure 2). Analysis of interaction pattern between protein and ligand during simulation shows the dynamic behaviour of each type of interactions with respect

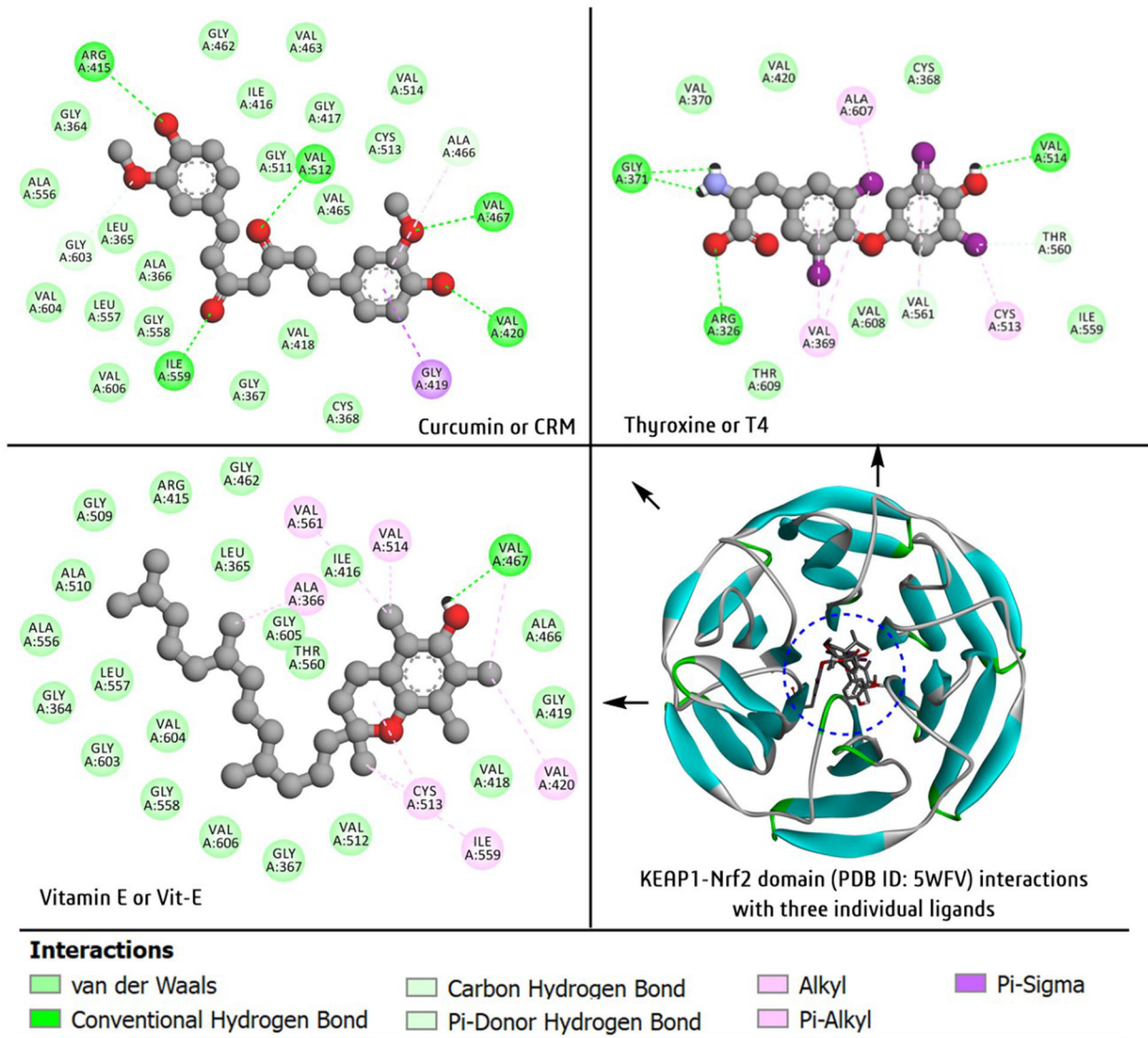


Figure 5. Molecular interaction of ligand-1, 2 and 3 against NRF-2 during docking study.

The ligands (thyroxine as ligand 1, vitamin E as ligand 2 and curcumin as ligand 3) were docked with the modeled human Nuclear factor erythroid 2-related factor (NRF-2) protein.

Table 2. Results of docking studies between the flanking region of genes and ligands.

Name of Gene	Ligand molecule	Number of polar bond at 3' or 5' promoter sites		Binding affinity at 3' or 5' promoter sites (in kcal/mol)	
		3' end	5' end	3' end	5' end
SOD1	Curcumin	4	4	-8.4	-8.5
	T4	5	4	-6.7	-6.7
	Vit-E	3	2	-6.6	-6.1
SOD2	Curcumin	1	3	-8.1	-8.2
	T4	3	3	-6.6	-6.8
	Vit-E	0	2	-6.9	-6.6
Catalase	Curcumin	2	4	-8.1	-8.3
	T4	4	7	-6.5	-6.9
	Vit-E	3	2	-6.7	-6.7
LDH	Curcumin	4	4	-7.1	-8.4
	T4	3	4	-6.5	-6.7
	Vit-E	1	3	-4.8	-6.5
NRF2	Curcumin	3	4	-8.2	-8.4
	T4	4	4	-6.7	-6.7
	Vit-E	0	0	-6.4	-6.2
Keap 1	Curcumin	4	4	-7.9	-8.2
	T4	6	5	-6.7	-6.7
	Vit-E	3	3	-5.9	-6.6

The docking was made between the flanking regions of the promoter site of the redox regulating genes (superoxide dismutase (SOD) 1 and 2 a i.e. CuZn and Mn SODs, respectively and catalase), Lactate Dehydrogenase (LDH) and redox enzyme signalling system (Nuclear factor erythroid 2-related factor 2, NRF-2 and Kelch-like ECH-associated protein 1, Keap 1) controlling molecules with the ligands i.e. curcumin, Thyroxin (T4), and Vitamin -E (VIT-E). As shown in the table the total polar bond for the interaction was presented along with their corresponding binding energy are presented.

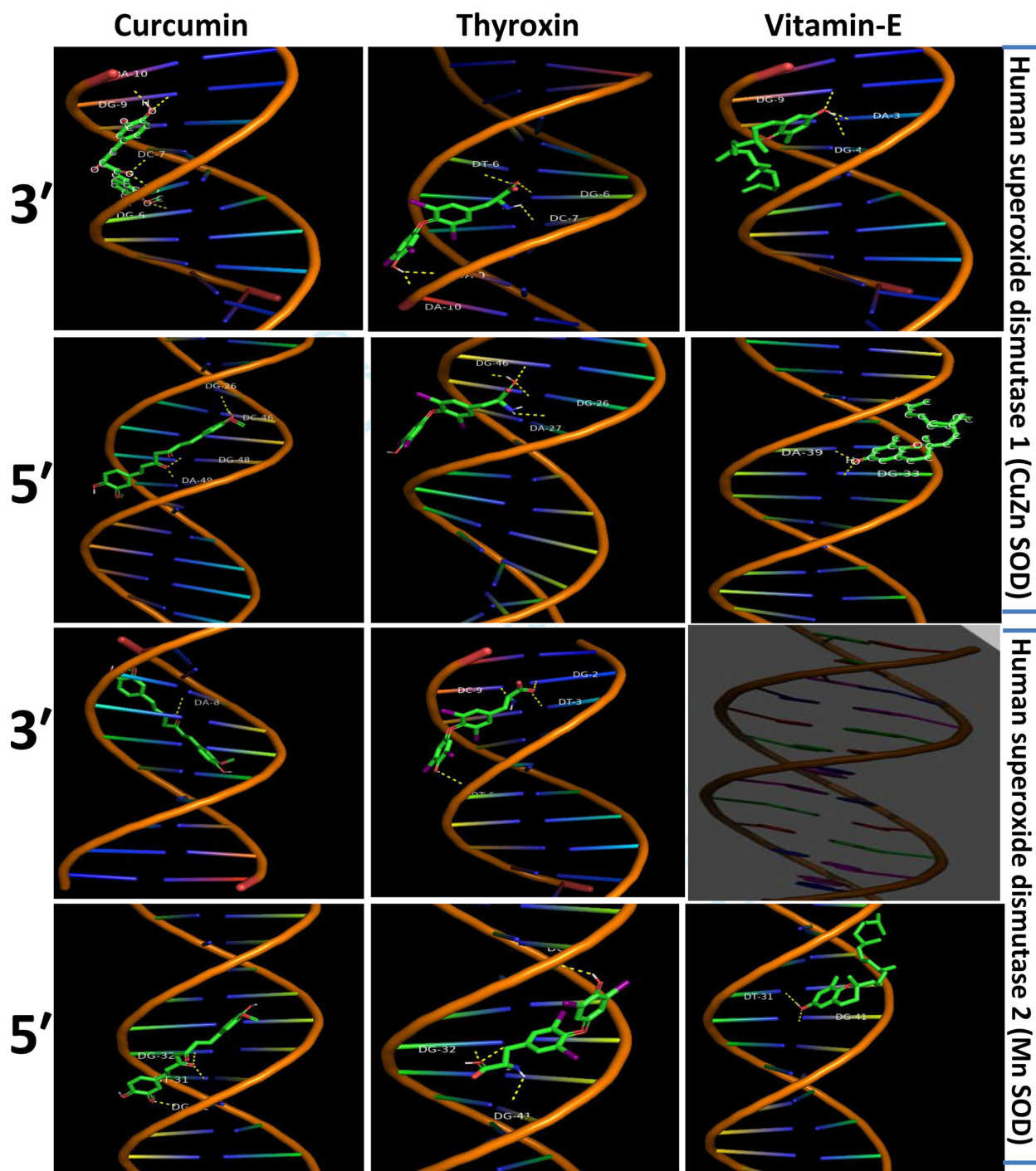


Figure 6. Docking between ligands and flanking region of the promoter site of human SOD1 and SOD2 genes.

Docking was done in the flanking regions of the promoters both at 3' and 5' site of human cytoplasmic superoxide dismutase (SOD) 1 i.e. CuZn SOD and SOD2 i.e. mitochondrial Mn SOD. The results of the docking studies with ligands such as curcumin, thyroxin and vitamin E were presented in column 1, 2 and 3, respectively. The brownish figure in 3' panel of SOD2 indicates no interaction with the ligand Vitamin E.

to time. Hydrophobic interaction was prominent between KEAP1 and VIT-E (Figure 9b). In addition to hydrophobic interactions there were water bridges. There was only one hydrogen bond between only hydroxyl group of VIT-E and backbone of Leu57. However, prominent hydrophobic interaction was negligible in KEAP1-CRM complex while there were 3 hydrogen bonds between CRM and KEAP1 (Figure 9d). CRM was also found to form many water bridges with protein while only one significant hydrophobic contact was observed with Val514.

3.1.4. Pharmacokinetics prediction

From predicted pharmacokinetic profiles, except CYP3A4 inhibitor and some variation in skin permeation or Log Kp value, CRM and T4 displayed similar types of profiles (Table 5). Nevertheless, CRM (-4.45 (1.31e-02) comparatively showed more water solubility than T4 (-6.79 (1.27e-04). At the same time, Vit-E showed different profiles, as low GI-absorption and P-gp substrate interaction without CYP2C9 inhibitor activity (Table 5).

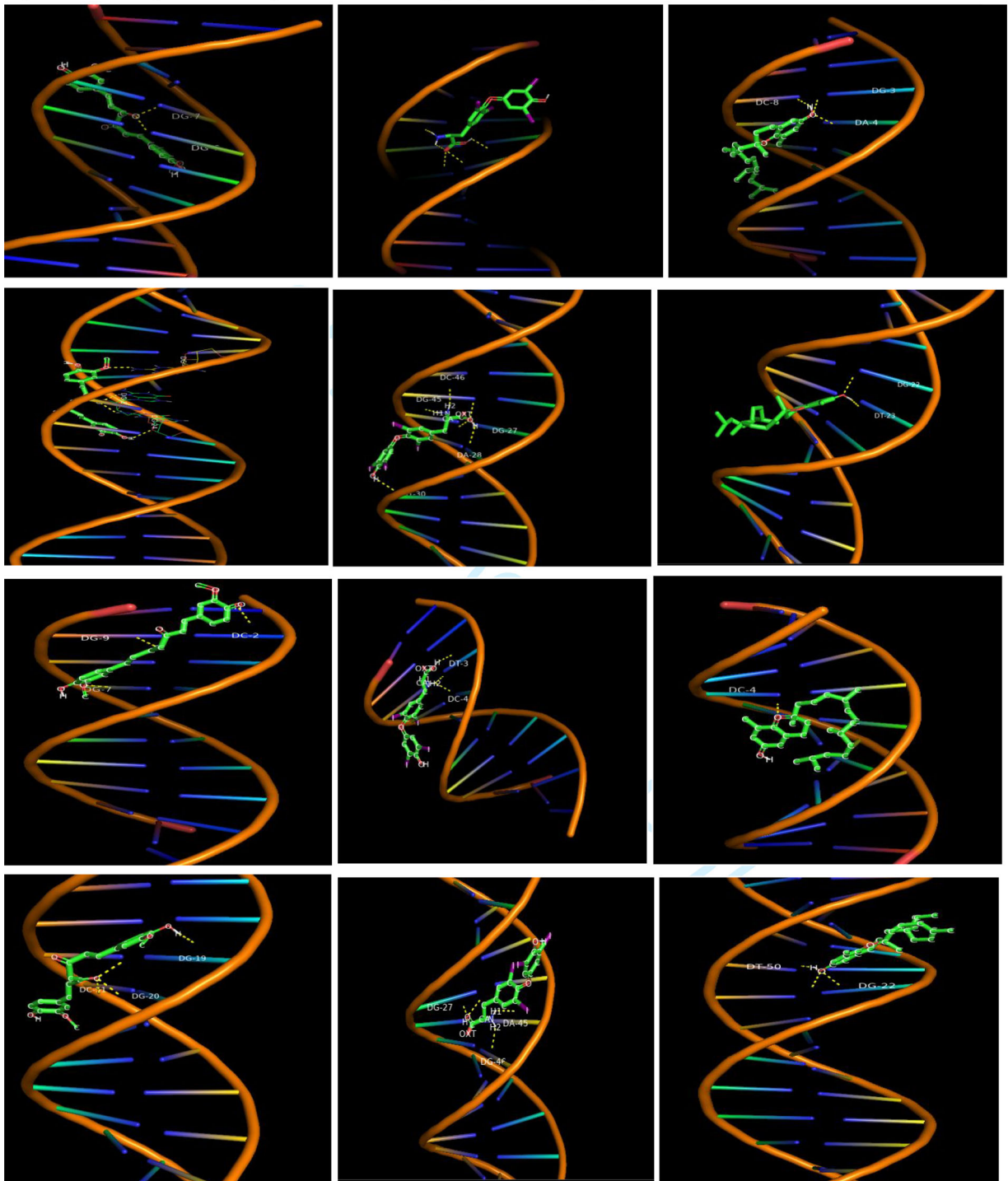


Figure 6. (Continued).

3.2. In vitro results

3.2.1. Cell viability assay (lactate dehydrogenase assay)

The release of LDH was same in all the T_4 treated groups either with or without co-treatment of vitamin E or/and CRM (Table 3) implying that all three ligands (T_4 , VIT-E and CRM) at the concentrations treated are non-cytotoxic.

3.2.2. Intracellular ROS

Compared to the control cells, T_4 treated cardiac cells exhibited a significant increase in cellular levels of ROS in the

absence of VIT-E or/and CRM. However, co-treatment with VIT-E or/and CRM prevented the production of intracellular ROS (Figure 10).

3.2.3. Mitochondrial membrane permeability

The MMP was elevated in the T_4 treated group which was attenuated by the administration of VIT-E or/and CRM and the magnitude of attenuation was comparable in all the three antioxidant treated groups (Figure 11).

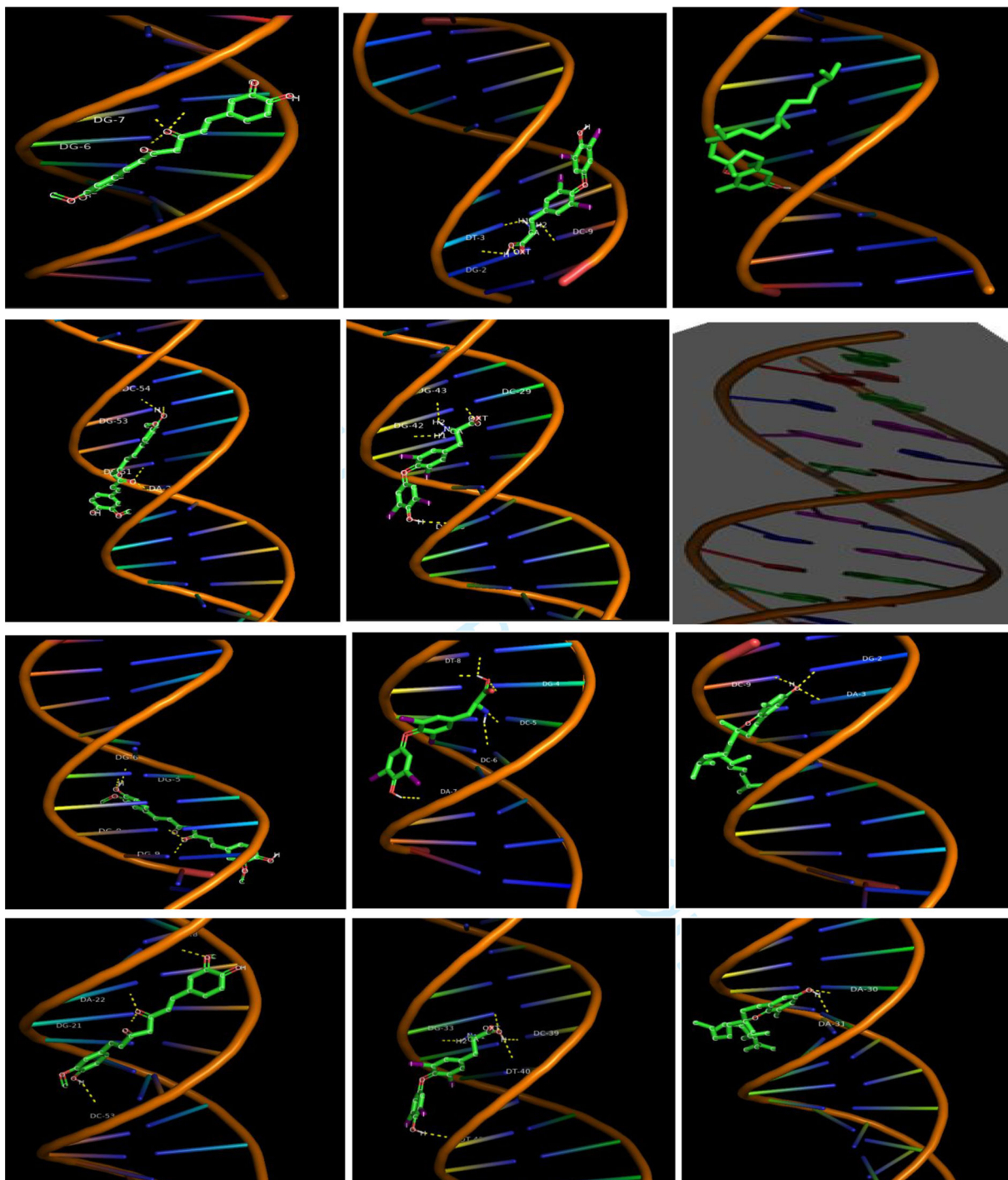


Figure 6. (Continued).

3.2.4. Membrane damage

Pilot studies showed that T_4 treatment induced free radical release after 30 min with a maximum burst at 4 h which subsequently declined after 6 h and brought back to control level by 24 h. Therefore, to test the efficacy of antioxidants the cells were pre-treated with VIT-E or/and CRM for 24 h followed by T_4 treatment for 4 h.

3.2.5. Lipid peroxidation

Endogenous LPx level in the membrane fractions of H9c2 cells was significantly elevated in the T_4 treated group (Gr II)

in the absence of any antioxidant supplementation. However, co-treatment of vitamin E or/and CRM along with T_4 prevented the T_4 treated group (Gr II) from damage due to LPx in a more or less similar manner (Table 3).

3.2.6. Activities of antioxidant enzymes

The SOD activity was increased in the T_4 treated group in the absence of any antioxidant treatment. It was observed that vitamin E or/and CRM were able to reduce this augmentation after 24 h (Table 3). The T_4 treatment resulted in the decrease in the CAT activity which was effectively reduced

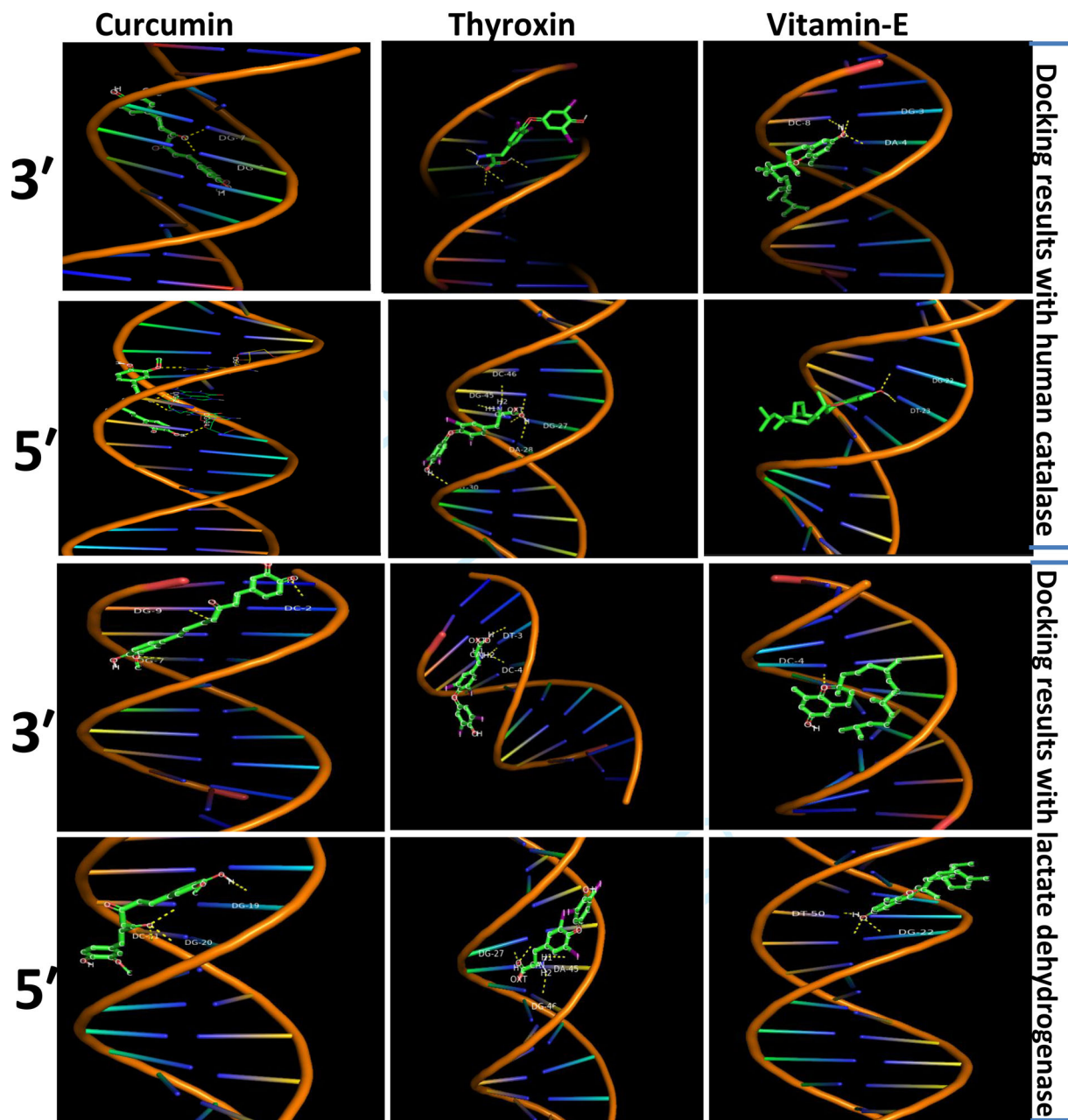


Figure 7. Docking between curcumin, thyroxin and vitamin E and flanking regions of the promoter sites of human catalase and LDH genes. Docking was done in the flanking regions of the promoters both at 3' and 5' site of human catalase gene and lactate dehydrogenase (LDH) genes. The results of the docking studies with ligands such as curcumin, thyroxin and vitamin E were presented in column 1, 2 and 3, respectively.

by pre-treatment of vitamin E or/and CRM after 24 h (Table 3).

3.3. DFA Analysis

The results obtained from the study are presented in Figure 12 and Table 4. All data sets such as the levels of intracellular ROS, MMP, LPx and the activities of the antioxidant enzymes were taken together for the DFA analyses. A discriminant function is a latent variable which is constructed as a linear combination of independent variables. A discriminant function is also known as canonical root used to classify the groups based on observed values of predictor variables. The numerical data of the control, T_4 , $T_4 + \text{VIT-E}$, $T_4 + \text{CRM}$ and

$T_4 + \text{VIT-E} + \text{CRM}$ group after DFA analyses indicate that T_4 group was well separated from the other groups. This implies the accurate action of the hormone and the compounds treated on the studied parameters. The pictorial representation of the outputs from DFA study (Figure 12b) surmises that the ellipses represent the 95% confidence limits for each of the groups. Groups that are superimposed in two dimensions (control and antioxidant treated) are more likely to be confused with one another while the T_4 group stands out separately. Especially, $T_4 + \text{VIT-E} + \text{CRM}$ group was at the extreme negative coordinate as compared to all the other groups. It indicates the distinct but synergetic effects of both VIT-E and CRM over the other groups as depicted in Table 4 representing the Standardized coefficient for

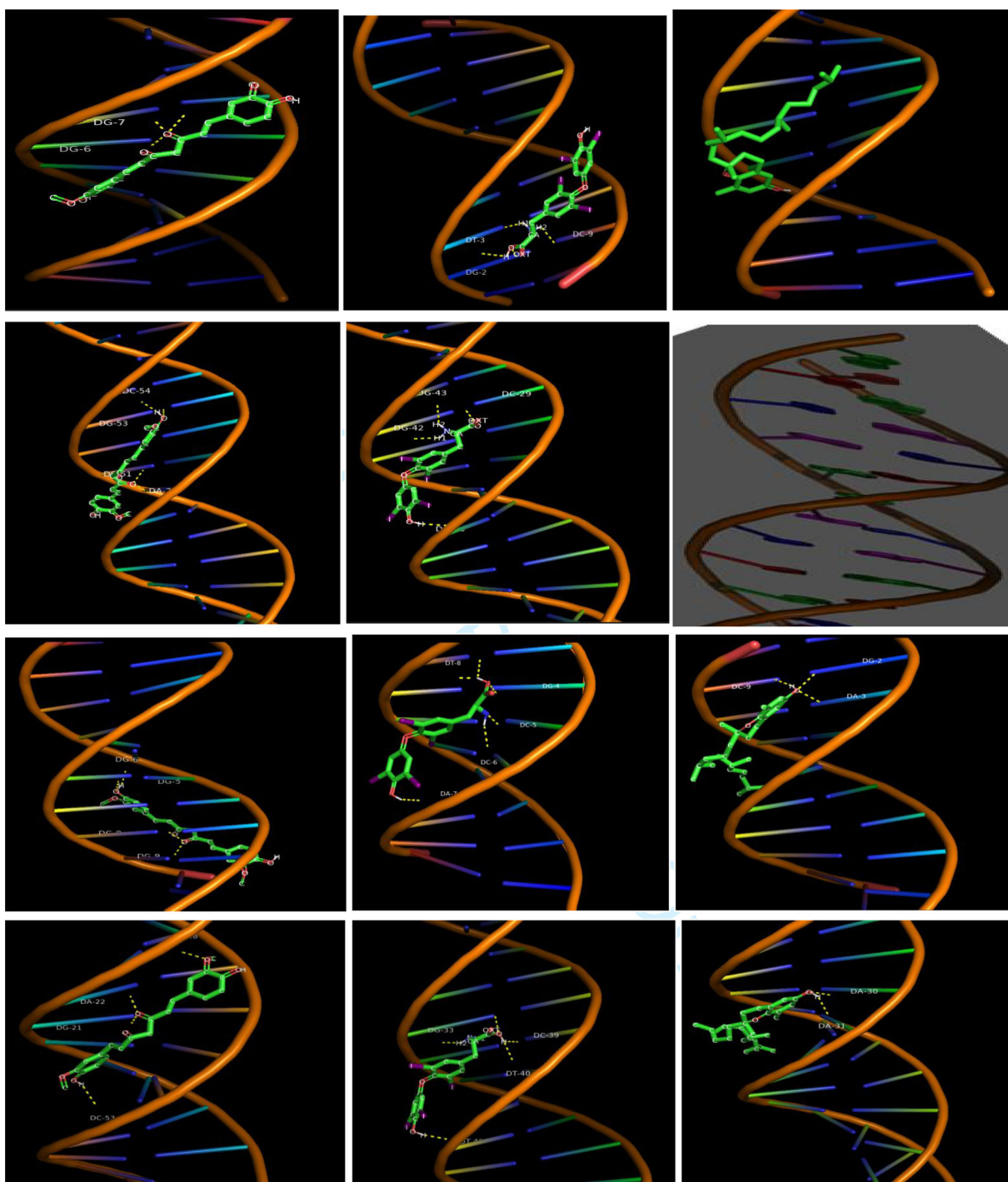


Figure 7. (Continued).

canonical variables for the individual parameters. The parameters responsible for segregation of the studied groups were LPx via root 1, SOD via root 2 and CAT via root 3 (Table 4) and therefore, were better predictors of the effects of the ligands, i.e. T4, VIT-E and CRM validating the results of the *in silico* docking studies (Figures 1–5).

4. Discussion

In our previous study, we showed the molecular interaction of a modelled active portion of the zipped protein NRF-2

with both VIT-E and CRM and the antioxidant complex (VIT-E & CRM) with NRF-2 (Mishra et al., 2019). NRF-2 is a redox-sensitive cytoplasmic inhibitor of the transcription factor NRF-2. Dissociation of the NRF-2 activates the NRF-2 for its translocation to the nucleus for upregulation of antioxidant response system (AREs). It could indicate the cardio-protective role of CRM against oxidative stress by increasing NRF-2 expression and decreasing NF-kB activation in both *in vivo* and *in vitro* models of mice hearts. In another study, it has been observed that vitamin E alleviates oxidative stress in cardiac cells by activating NRF-2 (Vineetha et al., 2018).

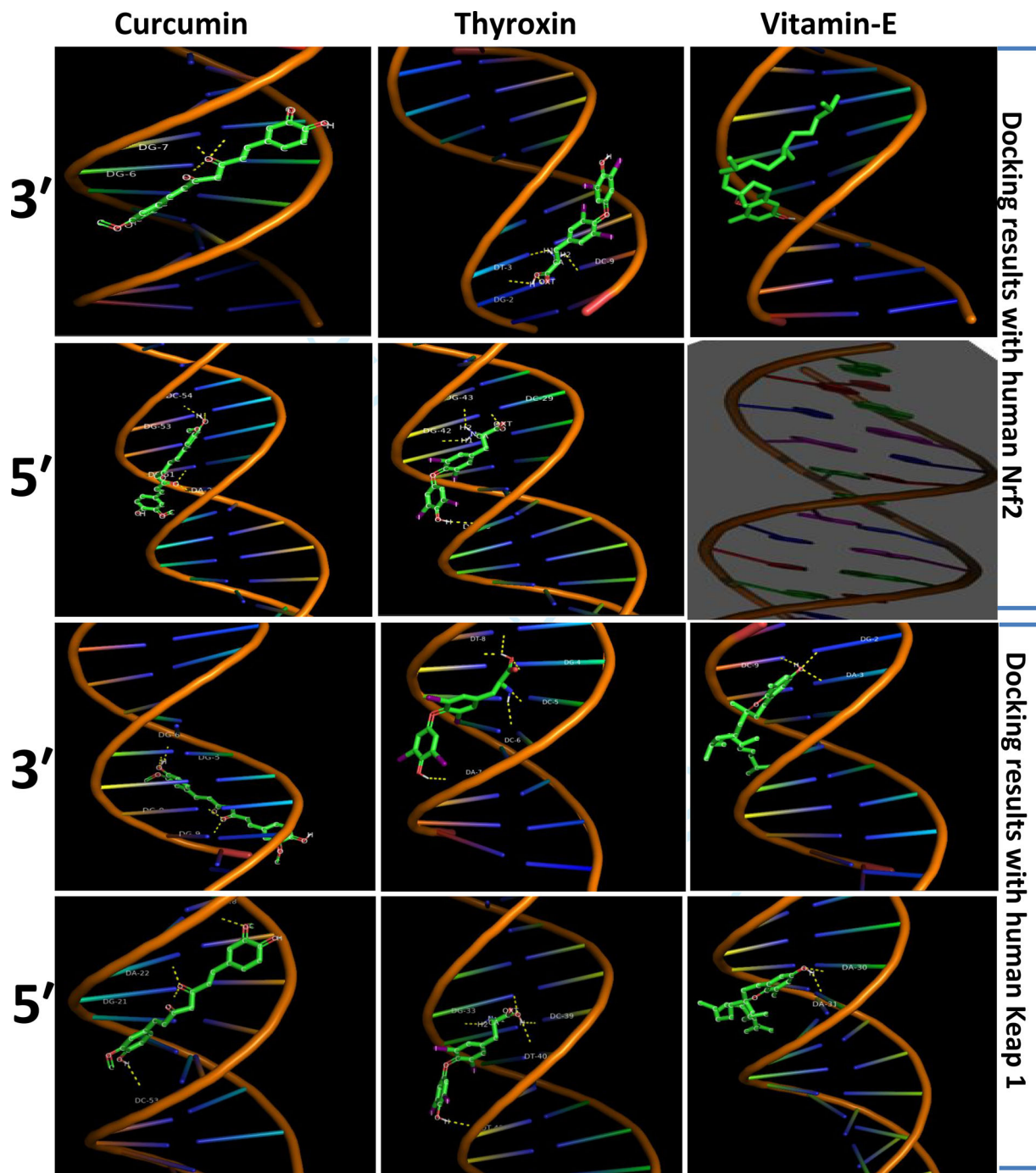


Figure 8. Docking between ligands and flanking region of the promoter site of human Keap 1 and NRF-2 genes.

Docking was done in the flanking regions of the promoters both at 3' and 5' site of human Kelch-like ECH-associated protein (Keap) 1 and human nuclear factor erythroid 2-related factor (NRF-2) genes. The results of the docking studies with ligands such as curcumin, thyroxin and vitamin E were presented in column 1, 2 and 3, respectively. The brownish figure in 5' panel of NRF-2 indicates no interaction with the ligand Vitamin E.

Costilla et al also observed that increase in ROS level in the hyperthyroid state induces the antioxidant enzyme transcription through the activation of the NRF-2 in lymphoid tissues (Costilla et al., 2019). Hence, all these studies indicate the protective role of CRM and vitamin E against oxidative stress in cardiac system.

Computational work is an ingenious approach, that not only reduces the required for laboratory validation, but also crafts the most effective and targeted approach (Swain et al., 2015). To establish the possible role of NRF-2 and NRF-2 signalling system on the ARE responses under TH stress, we have

tried to perform docking studies. The *in silico* docking was performed between the predicted or crystal structure models of mammalian redox regulatory enzymes available in PubMed (CAT, SOD, LDH), KELCH-KEAP1 domain and -KEAP1NRF 2 domain and the pharma/nutraceuticals (T4, CRM and VIT-E alone or in combination) as ligands. The score table indicates that KELCH-KEAP1 domain and KEAP1-NRF 2 are the most interactive proteins that showed high docking scores when docked with poly-ligands, i.e. VIT-E/CRM or VIT-E/CRM/T4, yet, the other redox molecules also had notable scores indicating their interactions with the ligands. In the present study, for

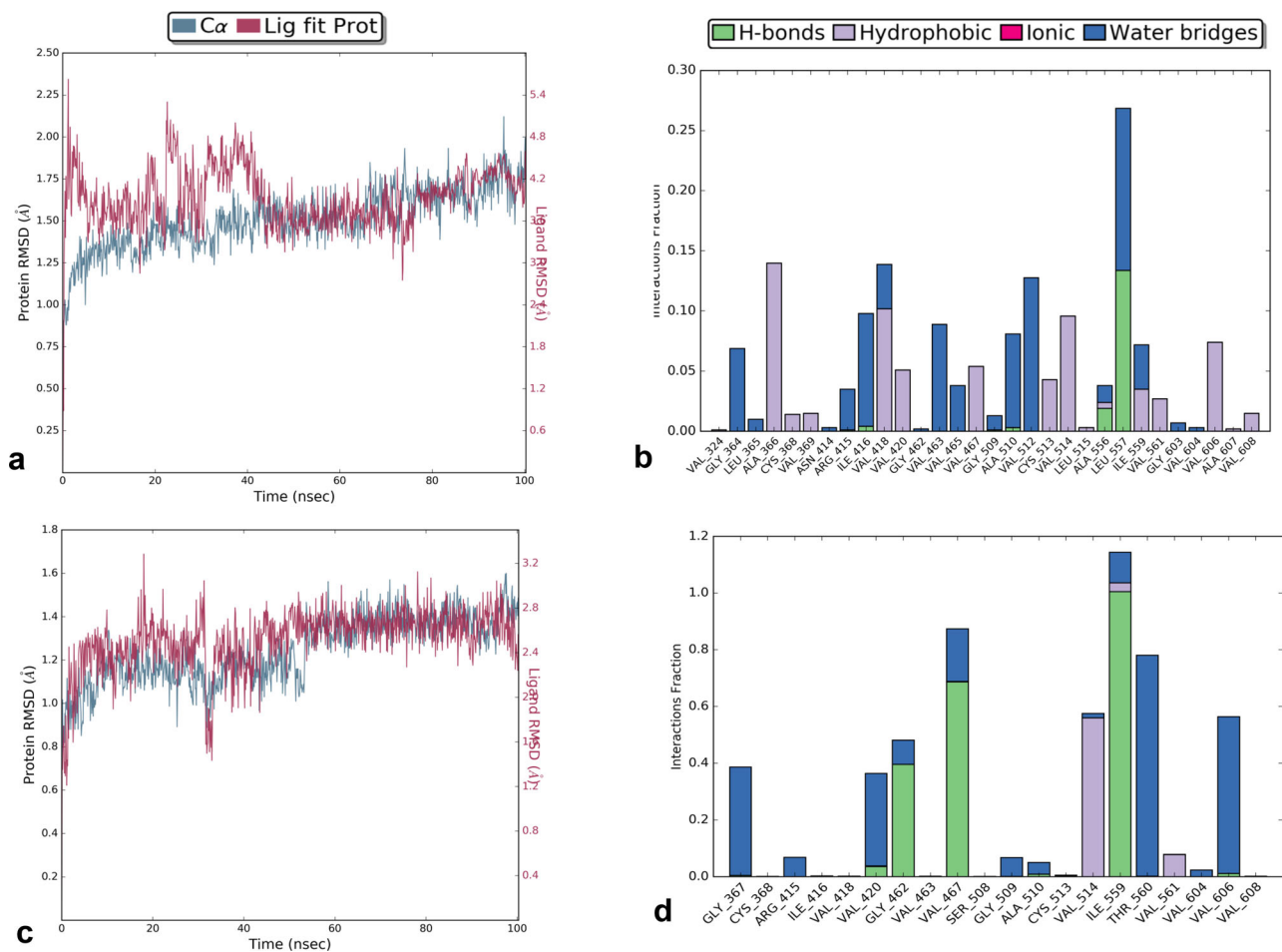


Figure 9. Root mean square deviation plot of (a) MD trajectory of KEAP1-VitE complex and (b) KEAP1-CRM complex with respect to time and interactions plot (c) between KEAP1-VitE and (d) KEAP1-CRM during MD simulation.

Table 3. Effects of vitamin E and curcumin on LPx, LDH leakage, activity of SOD and Catalase in various T₄ treated H9c2 cells. Data are expressed as mean \pm S.D of three independent observations carried out in triplicate. $p < 0.05$ and $*p < 0.05$ with respect to control and T₄ treatment respectively.

Parameters	Gr I (Control)	Gr II (T ₄)	Gr III (T ₄ +Vit E)	Gr IV (T ₄ +Cur E)	Gr V (T ₄ +Vit E + Cur)
LPx	2.3 \pm 0.3*	4.7 \pm 0.18 ^S	2.4 \pm 0.14*	2.8 \pm 0.3*	2.2 \pm 0.2*
LDH	0.24 \pm 0.02	0.26 \pm 0.01	0.22 \pm 0.01	0.23 \pm 0.01	0.22 \pm 0.01
SOD	13.8 \pm 1.8*	17.2 \pm 1.2 ^S	14.8 \pm 1.6*	14.2 \pm 2*	13.9 \pm 1.2*
CAT	0.26 \pm 0.02*	0.20 \pm 0.02 ^S	0.24 \pm 0.04* ^S	0.28 \pm 0.03*	0.28 \pm 0.03*

^S $p < 0.05$ with respect to control.

* $p < 0.05$ with respect to T₄ treatment.

Table 4. Linear discriminant analysis of oxidative stress parameters of five treatment groups of H9c2 cells.

Parameters	Root 1	Root 2	Root 3	Root 4
LPx	1.34128	-0.164207	0.223934	0.133696
LDH	0.78232	-0.772741	-0.642313	-0.224988
SOD	0.25929	0.850825	0.119530	-0.741424
CAT	-0.77916	-0.767172	0.536734	-0.290597
Eigenvalue	60.34785	0.877720	0.252583	0.001446
Cumulative Proportion	0.98159	0.995868	0.999976	1.000000

Loadings (eigenvectors) on four linear discriminant axes (roots) computed using four (principal component) biochemical variables. Largest values shown in bold. The bold values for the Standardized coefficient for canonical variables indicate the significant contribution of the respective parameter in discriminating the group from each other via the respective roots. LPx- Lipid peroxides, LDH- lactate dehydrogenase, SOD- superoxide dismutase, CAT- catalase.

the first time, we showed the modelled mammalian NRF-2 interaction with the ligands as an extension of our previous work using only the active part of NRF-2 due to technical limitations. This in depth analysis further substantiated the

proposed mechanism of activation of NRF-2 via KELCH-KEAP1 domain interaction to activate ARE in hyperthyroid rat heart to protect it from oxidative stress (Mishra et al., 2019). Since CRM has multifaceted physiological and cellular functions like

Table 5. Predicted pharmacokinetics profiles of CRM, Vit-E and T4 using SwissADME tool.

Parameters	Curcumin	vitamin E	Levothyroxine
GI-absorption	High	Low	High
BBB permeant	No	No	No
P-gp substrate	No	Yes	No
CYP1A2 inhibitor	No	No	No
CYP2C19 inhibitor	No	No	No
CYP2C9 inhibitor	Yes	No	Yes
CYP2D6 inhibitor	No	No	No
CYP3A4 inhibitor	Yes	No	No
Log K_p (skin permeation in cm/s)	-6.28	-1.33	-9.36
Log S (water solubility in mg/ml) class	-4.45 (1.31e-02) moderate soluble	-9.16 (2.97e-07) poorly soluble	-6.79 (1.27e-04) poorly soluble

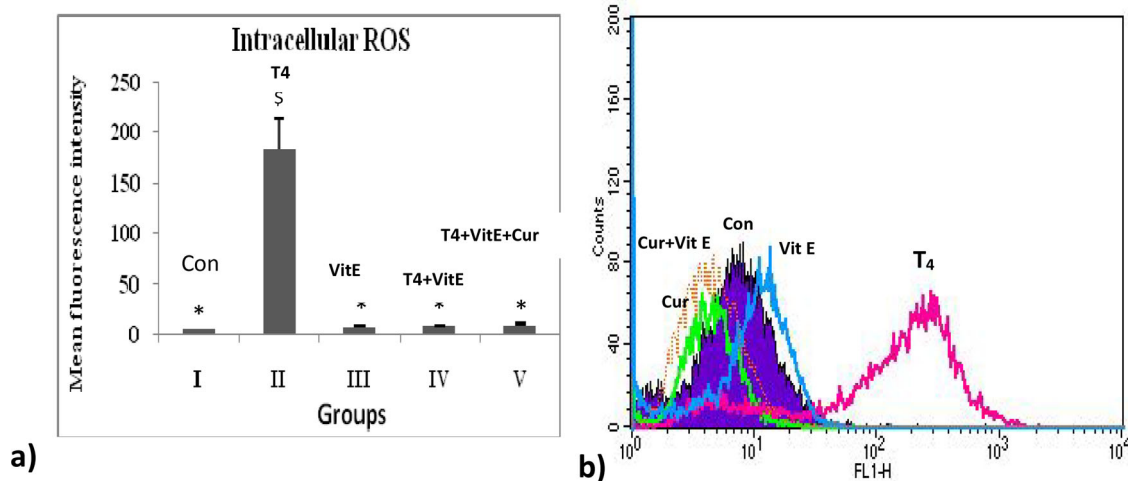


Figure 10. Effects of vitamin E or/and curcumin on T₄-induced intracellular ROS generation in various T₄ treated H9c2 cells. (a) ROS generation measured as DCFH-DA fluorescence (b) Representative graph of mean fluorescence intensity of ROS estimation as revealed by FACS analysis. Data are expressed as mean \pm S.D of three independent observations carried out in triplicate. \$p < 0.05\$ and * $p < 0.05$ with respect to control and T₄ treatment respectively. Groups; I (Con): Control; II: T₄; III (VIT-E): Vitamin E + T₄; IV (Cur): Curcumin + T₄; V (Cur + VIT-E): Vitamin E + Curcumin + T₄

antioxidant, antimicrobial and anticancer properties to name a few, it will not be out of context to mention that it will have multiple targets of action to elicit diverse effect. Similarly vitamin E is reported to have differential modulation of expression of multiple genes in different tissues, which suggested that changes in gene expression are reflective of tissue function and the tissue-specific regulation of vitamin E (Kim & Han, 2019). Therefore, to strengthen our hypothesis we further employed novel approach to compute the interaction between the ligands and the promoters of the studied redox regulating enzymes and other proteins including NRF-2, KELCH and KEAP1.

Interaction of the promoter sites with the ligands (T₄, VIT-E and CRM) *in silico* revealed that the studied ligands modulate the expressions of the target genes (SOD1, SOD2, CAT, LDH, KELCH-KEAP 1 domain and KEAP1-NRF 2 domain). Docking results surmise that CRM had the most interactive score followed by T₄ while VIT-E had the lowest score is rather a silent one. Amongst the various groups present on the ligands, as expected C=O group followed by OH group were the most reactive ones as they were involved in stabilizing the interactions among the partners.

Comparative analysis of r. m. s deviation plot of KEAP1 complexed with VIT-E and CRM reveals that binding of CRM with KEAP1 is more stable compared to VIT-E (Figure 9). This is mainly due to strong polar interactions between hydroxyl groups of CRM and protein atoms whereas VIT-E lacks such

polar groups because of its hydrophobic nature. This was further corroborated by the presence of several hydrophobic interactions between VIT-E and KEAP1 while presence of several hydrogen bonds between CRM and KEAP1. Also, one remarkable observation was that most of the interactions between KEAP1 and VIT-E was found to be present for less than 30% of trajectory during simulation period whereas majority of prominent interactions with CRM were observed in more than 50% MD trajectory during simulation.

Pharmacokinetics prediction indicates that CRM showed ideal profiles than Vit-E, like T₄ mainstream drug. Overall, all three drugs are expected to maintain the perfect pharmacokinetics profiles during oral administering in synergy. In traditional cases, pharmacokinetics profile was predicted in late-stage drug discovery with inexpensive *in vitro* and *in vivo* methods without prior information. Indeed, in advance prediction through the computational tool is a more resource and time-saving approach for current drug development.

Overall, *in silico* docking with either redox regulatory or sensing proteins or their genes with the ligands, give further clue to control the hyperthyroid induced oxidative stress synergistically by co-administration of CRM and VIT-E in cardiac system. Thyroid hormone receptor (TR) α and β are ligand-inducible nuclear receptors/transcription factors responsible for eliciting the effects of TH on the target cells (Kim & Mohan, 2013). Therefore, it's not

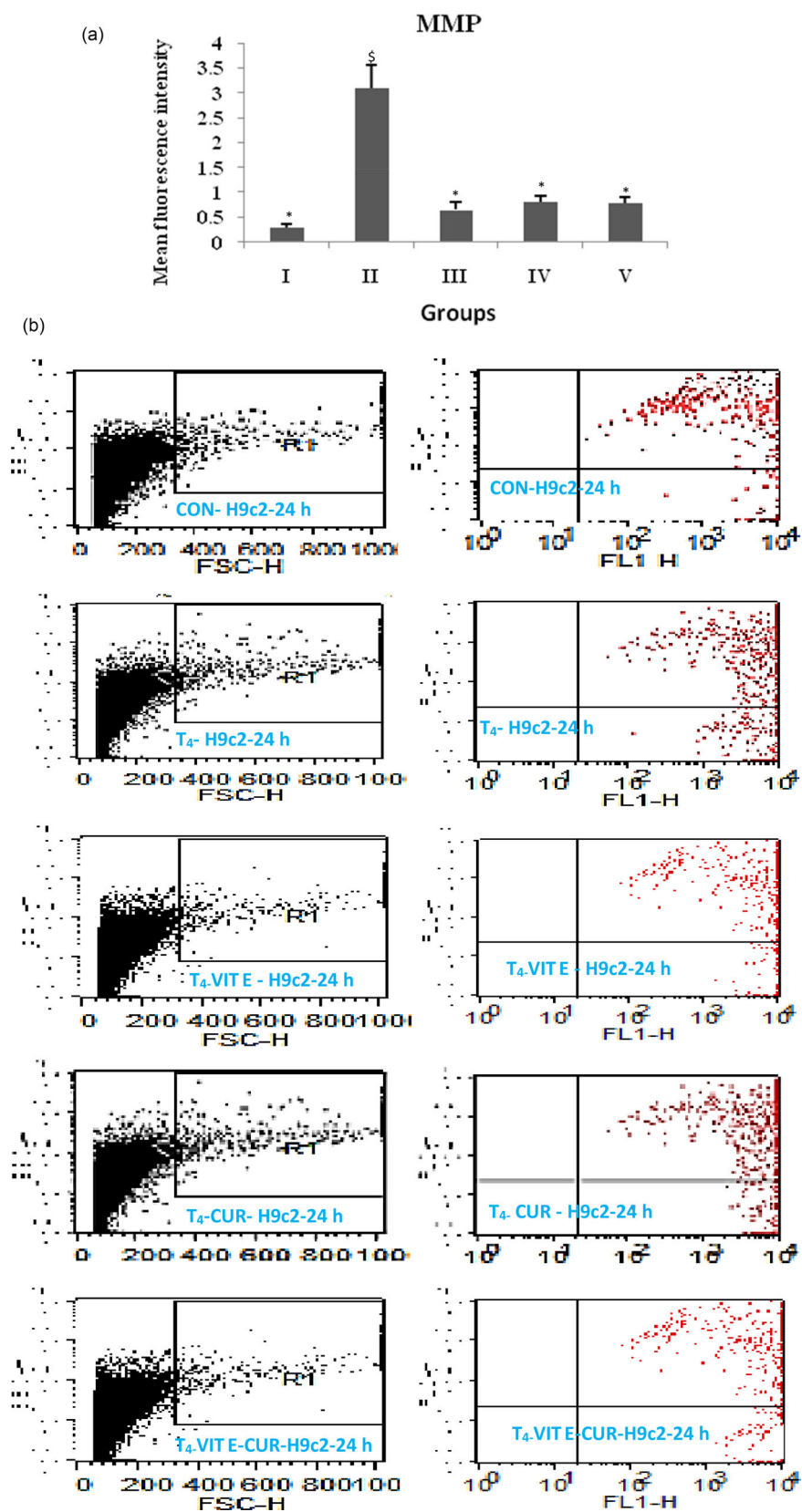


Figure 11. Effect of vitamin E or/and curcumin on T_4 -induced alteration in MMP in various T_4 treated H9c2 cells. (A) Estimation of MMP by the uptake of a membrane potential-sensitive fluorescence dye JC-1 using FACS analysis. (B) Representative graph of mean fluorescence intensity of MMP estimation as revealed by FACS analysis. Data are expressed as mean \pm S.D of three independent observations carried out in triplicate. $^{\$}p < 0.05$ and $^*p < 0.05$ with respect to control and T_4 treatment respectively.

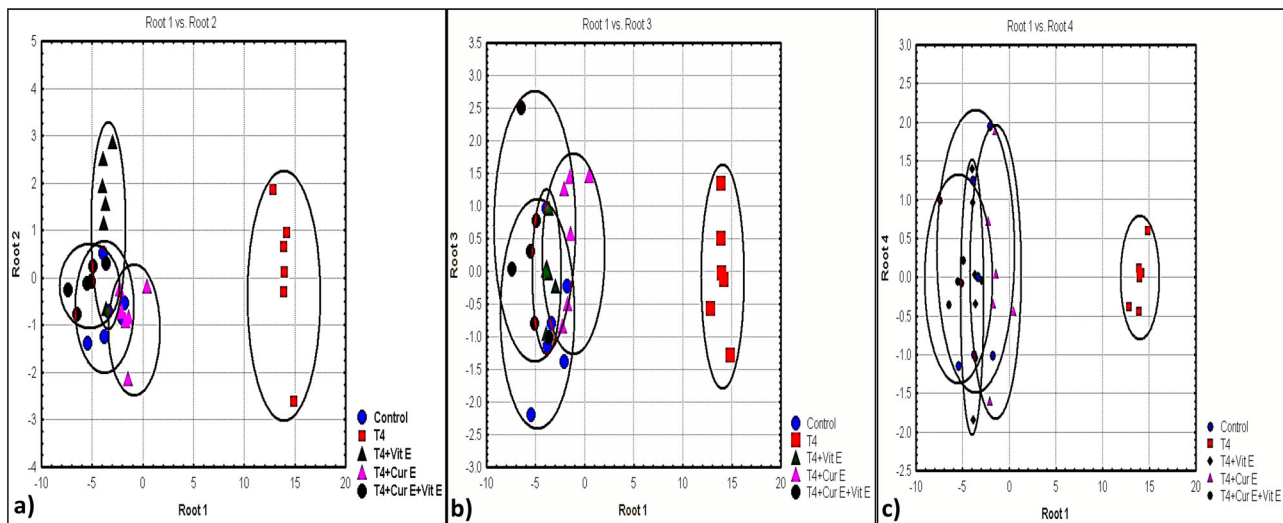


Figure 12. Discriminant function analysis of the studied biochemical parameters as a function of treatment groups.

Individual data set of the studied biochemical parameters (LPx, activities of SOD, CAT, LDH and MMP level) in control, Thyroxin (T_4), T_4 + Vitamin- E (VIT-E), T_4 + Curcumin and T_4 +VIT-E + curcumin were subjected to discriminant function analyses. The outputs via all the roots such as root 1 versus root 2 (a), root 2 versus root 3 (b) and root 1 versus root 4 (c) were presented in the figure. The control group was clearly separated as compared to others indicating definite effects of the treated molecules including T_4 . Although the groups among the treatment with curcumin and/or VIT-E were intermingled with each other, a slight difference among them was noticed indicating their individual and synergetic effects to combat T_4 induced changes on the studied above biochemical parameters in the cells. The protective effects of both VIT-E and curcumin together are better indicated from the Table 2 presenting the Standardized coefficient for canonical variables for the individual parameters.

surprising to notice it as a good ligand for other promoters. However, its ability to bind with the promoter sites of redox regulatory enzymes as reported in the present study definitely shed light on the induced oxidative stress condition under hyperthyroidism. Our results on promoter docking with CRM indicates that this multipotent nutraceutical is capable of eliciting powerful positive pharmacological effects by interacting with the promoters as well as direct interaction with the target proteins. It will not be out of context to mention here that previous reports also advocate for CRM and DNA interactions via UV analysis and Fourier transform infrared (FTIR). The authors showed that CRM has the ability to bind with both the minor and major grooves of the DNA duplex, the backbone phosphate group as well as with the RNA base (Nafisi et al., 2009) without inducing any conformational change. It is further revealed from their study that that CRM binds to the minor groove via thymine O_2 while its binding to the major groove and the backbone phosphate group is facilitated by guanine and adenine N7.

On the other hand, uracil O_2 is responsible for RNA binding whereas guanine and adenine N7 atoms help CRM interact with the backbone phosphate group. Above all the authors showed that the binding of CRM with DNA was stronger in comparison to binding with RNA. Our results further corroborated the findings that the binding of CRM with promoter site DNA is principally via $C=O$ and OH group. This hypothesis is further corroborated with the in vitro data using cardiac H9C2 cell line where the T_4 -induced oxidative stress as evidenced by induction of ROS generation and LPx, alteration of MMP and activities of SOD and CAT which was ameliorated with CRM and VIT-E treatment.

Discriminant function analysis (DFA) is a multivariate test of differences between groups and uses data-reduction technique to make decisions to determine the minimum number of dimensions needed to describe these differences

(Mohanty & Samanta, 2016; Paital & Chainy, 2010, 2012, 2013a, b). In this case, the contribution of any variables studied (e.g. ROS generation, MMP, LPx, SOD and CAT activities) on differentiation of groups or effects of the experimental components (i.e. T_4 , VIT-E, CRM and VIT-E + CRM) were studied using DFA. All sets of the obtained data including the titre of LPx, activities of the SOD, CAT and LDH and the intensity of MMP have yielded 5 groups, indicating the definite effects of the neutra/pharmaceuticals used on the redox metabolism in cardiac cell lines. This was evidenced by the separation of the control group into a clear separation from the rest of the studied groups. The fact is clear via root 1 versus rest of the roots i.e. root 2, 3 and 4. The term root refers to the Eigen values that are associated with the respective canonical function.

The maximum number of functions is equal to the number of groups minus one ($5-1=4$), or the number of variables in the analysis, whichever is smaller. This also implies the precise action of the hormone T_4 and the compounds treated to restore the oxidative stress metabolism into normal conditions in the H9C2 cardiac cell line. The recovery treatment groups such as T_4 + VIT-E, T_4 + CRM and T_4 + VIT-E + CRM were having a trend of shifting towards the negative coordinate along the root 1 via root 2, 3 and 4. Especially, later group i.e. T_4 + VIT-E + CRM group was found to be placed at the extreme negative coordinate in comparison to all the other groups. It confirms that overall analyses of the data gave a clue about the synergetic effects of both VIT-E and CRM to restore the redox balance when treated together in compared to individual administration to the T_4 treated cardiac cells (Mishra et al., 2019). The values of the Standardized coefficient for canonical variables as indicated from their numerical values also substantiate the above fact. Albeit, the cumulative analysis indicate the protective effects of both VIT-E and CRM, an in depth discussion on individual parameters would help in understanding the proposed

hypothesis. The canonical model of DFA implies the LPx and LDH via root 1, SOD via root 2 and CAT via root 3 were key parameters responsible for the separation of the studied groups into 5 and can be used as predictors of T4-induced oxidative stress as well as ameliorative effects of CRM and VIT-E as synergists.

5. Conclusion

The results of *in silico* analysis suggest the multi-targeted impact of CRM at transcription and protein level activates NRF-2 by releasing NRF-2, thereby activates ARE under hyperthyroid stress. Further, VIT-E and CRM co-treatment had synergistic effect despite VIT-E being identified as a silent ligand for the genes/proteins studied. This may be attributed to non-genomic impacts of VIT-E. Restoration of the T4-induced augmented levels of biochemical markers such as levels of LPx, ROS, and activities of enzymes such as SOD, CAT, LDH and MMP to basal level by CRM and VIT-E also supported the above finding.

Disclosure statement

No potential conflict of interest was reported by the authors.

Funding

The work was funded by fellowship provided to PM under RFSMS scheme, UGC, New Delhi and Schemes number ECR/2016/001984 by SERB, DST, Govt. of India and 1188/ST, Bhubaneswar, dated 01.03.17, ST-(Bio)-02/2017, DST, Govt. of Odisha provided to BRP.

ORCID

Pallavi Mishra  <http://orcid.org/0000-0002-3776-3971>
 Gitanjali Tandon  <http://orcid.org/0000-0002-9832-0488>
 Manoj Kumar  <http://orcid.org/0000-0002-8239-7253>
 Biswaranjan Paital  <http://orcid.org/0000-0002-5285-6578>
 Shasanka Sekhar Swain  <http://orcid.org/0000-0001-5089-8304>
 Sunil Kumar  <http://orcid.org/0000-0001-9411-3863>
 Luna Samanta  <http://orcid.org/0000-0002-2969-0071>

References

Aebi, H. Catalase. (1974). In Bergmayer HU (Ed.), *Methods of enzymatic analysis* (Vol II, pp. 673–683). Academic press.

Afsar, B., Yilmaz, M. I., Siriopol, D., Unal, H. U., Saglam, M., Karaman, M., Gezer, M., Sonmez, A., Eyiletan, T., Aydin, I., Hamcan, S., Oguz, Y., Covic, A., & Kanbay, M. (2017). Thyroid function and cardiovascular events in chronic kidney disease patients. *Journal of Nephrology*, 30(2), 235–242. <https://doi.org/10.1007/s40620-016-0300-y>

Aggarwal, B. B., & Harikumar, K. B. (2009). Potential therapeutic effects of curcumin, the anti-inflammatory agent, against neurodegenerative, cardiovascular, pulmonary, metabolic, autoimmune and neoplastic diseases. *The International Journal of Biochemistry & Cell Biology*, 41(1), 40–59. <https://doi.org/10.1016/j.biocel.2008.06.010>

Ahmed, S. M., Luo, L., Namani, A., Wang, X. J., & Tang, X. (2017). NRF-2 signaling pathway: Pivotal roles in inflammation. *Biochimica et Biophysica Acta (BBA) - Molecular Basis of Disease*, 1863(2), 585–597. <https://doi.org/10.1016/j.bbadis.2016.11.005>

Araujo, A. S. R., Schenkel, P., Enzweiler, A. T., Fernandes, T. R. G., Partata, W. A., Llesuy, S., Ribeiro, M. F. M., Khaper, N., Singal, P. K., & Belló-Klein, A. (2008). The role of redox signaling in cardiac hypertrophy induced by experimental hyperthyroidism. *Journal of Molecular Endocrinology*, 41(6), 423–430. <https://doi.org/10.1677/JME-08-0024>

Bano, A., Chaker, L., de Maat, M. P. M., Atiq, F., Kavousi, M., Franco, O. H., Mattace-Raso, F. U. S., Leebeek, F. W. G., & Peeters, R. P. (2019). Thyroid Function and Cardiovascular Disease: The Mediating Role of Coagulation Factors. *The Journal of Clinical Endocrinology and Metabolism*, 104(8), 3203–3212. <https://doi.org/10.1210/jc.2019-00072>

Bowers, K. J., Chow, D. E., Xu, H., Dror, R. O., Eastwood, M. P., Gregersen, B. A., Klepeis, J. L., Kolossvary, I., Moraes, M. A., Sacerdoti, F. D. & Salmon, J. K. (2006). Scalable Algorithms for Molecular Dynamics Simulations on Commodity Clusters. *Proceedings of the 2006 ACM/IEEE Conference on Supercomputing (SC06)*, Tampa, FL, 11 to 17 November 2006. New York : ACM Press.

Bradford, M. M. (1976). A rapid and sensitive method for the quantification of microgram quantities of protein utilizing the principle of protein-dye binding. *Analytical Biochemistry*, 72(1-2), 248–254. [https://doi.org/10.1016/0003-2697\(76\)90527-3](https://doi.org/10.1016/0003-2697(76)90527-3)

Cabaud, P. G., & Wroblewski, F. (1958). Colorimetric measurement of lactic dehydrogenase activity of body fluids. *American Journal of Clinical Pathology*, 30(3), 234–236. <https://doi.org/10.1093/ajcp/30.3.234>

Cohen, G., Dembiec, D., & Marcus, J. (1970). Measurement of catalase activity in tissue extracts. *Analytical Biochemistry*, 34(1), 30–38. [https://doi.org/10.1016/0003-2697\(70\)90083-7](https://doi.org/10.1016/0003-2697(70)90083-7)

Costilla, M., Macri Delbono, R., Klecha, A., Cremaschi, G. A., & Barreiro Arcos, M. L. (2019). Oxidative Stress Produced by Hyperthyroidism Status Induces the Antioxidant Enzyme Transcription through the Activation of the NRF-2 Factor in Lymphoid Tissues of Balb/c Mice. *Oxidative Medicine and Cellular Longevity*, 2019, 7471890. <https://doi.org/10.1155/2019/7471890>

da Rosa Araujo, A. S., Silva de Miranda, M. F., de Oliveira, U. O., Fernandes, T., Llesuy, S., Rios Kucharski, L. C., Khaper, N., & Belló-Klein, A. (2010). Increased resistance to hydrogen peroxide-induced cardiac contracture is associated with decreased myocardial oxidative stress in hypothyroid rats. *Cell Biochemistry and Function*, 28(1), 38–44. <https://doi.org/10.1002/cbf.1616>

Das, K., Samanta, L., & Chainy, G. B. N. (2000). A modified spectrophotometric assay of superoxide dismutase using nitrite formation of superoxide radicals. *Indian J Biochemistry and Biophysics*, 37, 201–204.

DeLano, W. L. (2002). Pymol: An open-source molecular graphics tool. *CCP4 Newsletter on Protein Crystallography*, 40(1), 82–92.

Garg, S., Khan, S.I., Malhotra, R.K., Sharma, M. K., Kumar, M., Kaur, P., Nag, T. C., RumaRay, Bhatia, J., & Arya, D. S. (2020). The molecular mechanism involved in cardioprotection by the dietary flavonoid fisetin as an agonist of PPAR- γ in a murine model of myocardial infarction. *Archives of Biochemistry and Biophysics*, 694, 108572. <https://doi.org/10.1016/j.abb.2020.108572.E>

Gupta, S. C., Sung, B., Kim, J. H., Prasad, S., Li, S., & Aggarwal, B. B. (2013). Multitargeting by turmeric, the golden spice: From kitchen to clinic. *Mol Nutr Food Res*, 57(9), 1510–1528. <https://doi.org/10.1002/mnfr.201100741>

Haglund, T. A., Rajasekaran, N. S., Smood, B., Giridharan, G. A., Hoopes, C. W., Holman, W. L., Mauchley, D. C., Prabhu, S. D., Pamboukian, S. V., Tallaj, J. A., Rajapreyar, I. N., Kirklín, J. K., & Sethu, P. (2019). Evaluation of flow-modulation approaches in ventricular assist devices using an in-vitro endothelial cell culture model. *The Journal of Heart and Lung Transplantation : The Official Publication of the International Society for Heart Transplantation*, 38(4), 456–465. <https://doi.org/10.1016/j.healun.2018.10.007>

Hanwell, M. D., Curtis, D. E., Lonie, D. C., Vandermeersch, T., Zurek, E., & Hutchison, G. R. (2012). Avogadro: An advanced semantic chemical editor, visualization, and analysis platform. *Journal of Cheminformatics*, 4(1), 17. <https://doi.org/10.1186/1758-2946-4-17>

He, L., He, T., Farrar, S., Ji, L., Liu, T., & Ma, X. (2017). Antioxidants maintain cellular redox homeostasis by elimination of reactive oxygen species. *Cellular Physiology and Biochemistry : international Journal of Experimental Cellular Physiology, Biochemistry, and Pharmacology*, 44(2), 532–553. <https://doi.org/10.1159/000485089>

- Hercberg, S., Galan, P., Preziosi, P., Alfarez, M. J., & Vazquez, C. (1998). The potential role antioxidant vitamins in preventing cardiovascular diseases and cancers. *Nutrition (Burbank, Los Angeles County, Calif.)*, 14(6), 513–520. [https://doi.org/10.1016/S0899-9007\(98\)00040-9](https://doi.org/10.1016/S0899-9007(98)00040-9)
- Hunter, J. J., & Chien, K. R. (1999). Signaling pathways for cardiac hypertrophy and failure. *The New England Journal of Medicine*, 341(17), 1276–1283. <https://doi.org/10.1056/NEJM199910213411706>
- Jorgensen, W. L., Maxwell, D.S. & Tirado-Rives, J. (1996). Development and Testing of the OPLS All-Atom Force Field on Conformational Energetics and Properties of Organic Liquids. *Journal of American Chemical Society*, 118, 11225–11236.
- Kim, H. K., & Han, S. N. (2019). Vitamin E: Regulatory role on gene and protein expression and metabolomics profiles. *IUBMB Life*, 71(4), 442–455. <https://doi.org/10.1002/iub.2003>
- Kim, H. Y., & Mohan, S. (2013). Role and Mechanisms of Actions of Thyroid Hormone on the Skeletal Development. *Bone Research*, 1(2), 146–161. <https://doi.org/10.4248/BR201302004>
- Kim, S., Thiessen, P. A., Bolton, E. E., Chen, J., Fu, G., Gindulyte, A., Han, L., He, J., He, S., Shoemaker, B. A., Wang, J., Yu, B., Zhang, J., & Bryant, S. H. (2016). PubChem substance and compound databases. *Nucleic Acids Research*, 44(D1), D1202–213. <https://doi.org/10.1093/nar/gkv951>
- Klein, I. (1990). Thyroid hormone and the cardiovascular system. *The American Journal of Medicine*, 88(6), 631–637. [https://doi.org/10.1016/0002-9343\(90\)90531-H](https://doi.org/10.1016/0002-9343(90)90531-H)
- Kumar, M., Dahiya, S., Sharma, P., Sharma, S., Singh, T.P., Kapil, A., & Kaur, P. (2015). Structure based in silico analysis of quinolone resistance in clinical isolates of Salmonella Typhi from India. *PLoS One*, 10(5), e0126560. <https://doi.org/10.1371/journal.pone.0126560>
- Kuzman, J. A., O'Connell, T. D., & Gerdes, A. M. (2007). Rapamycin prevents Thyroid hormone-induced cardiac hypertrophy. *Endocrinology*, 148(7), 3477–3484. <https://doi.org/10.1210/en.2007-0099>
- Li, H. L., Liu, C., de Couto, G., Ouzounian, M., Sun, M., Wang, A. B., Huang, Y., He, C. W., Shi, Y., Chen, X., Nghiem, M. P., Liu, Y., Chen, M., Dawood, F., Fukuoka, M., Maekawa, Y., Zhang, L., Leask, A., Ghosh, A. K., Kirshenbaum, L. A., & Liu, P. P. (2008). Curcumin prevents and reverses murine cardiac hypertrophy. *Journal Clinical Investigations*, 118, 879–893.
- Li, L., Luo, W., Qian, Y., Zhu, W., Qian, J., Li, J., Jin, Y., Xu, X., & Liang, G. (2019). Luteolin protects against diabetic cardiomyopathy by inhibiting NF- κ B-mediated inflammation and activating the Nrf2-mediated antioxidant responses. *Phytomedicine : international Journal of Phytotherapy and Phytopharmacology*, 59, 152774 <https://doi.org/10.1016/j.phymed.2018.11.034>
- Li, D., Saldeen, T., & Mehta, J. L. (2000). Effects of alpha-tocopherol on ox-LDL-mediated degradation of IkappaB and apoptosis in cultured human coronary artery endothelial cells. *J Cardiovasc Pharmacol*, 36(3), 297–301. <https://doi.org/10.1097/00005344-200009000-00003>
- Mishra, P., Paital, B., Jena, S., Swain, S. S., Kumar, S., Yadav, M. K., Chainy, G. B. N., & Samanta, L. (2019). Possible activation of NRF2 by Vitamin E/Curcumin against altered thyroid hormone induced oxidative stress via NF κ B/AKT/mTOR/KEAP1 signalling in rat heart. *Scientific Reports*, 9 (1), 7408–7425. <https://doi.org/10.1038/s41598-019-43320-5>
- Mishra, P., & Samanta, L. (2012). Oxidative stress and heart failure in altered thyroid states. *TheScientificWorldJournal*, 2012, 741861. <https://doi.org/10.1100/2012/741861>
- Mohanty, D., & Samanta, L. (2016). Multivariate analysis of potential biomarkers of oxidative stress in Notopterus notopterus tissues from Mahanadi River as a function of concentration of heavy metals. *Chemosphere*, 155, 28–38. doi: 10.1016/2016.04.035.
- Nafisi, S., Adelzadeh, M., Norouzi, Z., & Sarbolouki, M. N. (2009). Curcumin binding to DNA and RNA. *DNA and Cell Biology*, 28(4), 201–208. <https://doi.org/10.1089/dna.2008.0840>
- Nguyen, T., Nioi, P., & Pickett, C. B. (2009). The NRF-2-antioxidant response element signaling pathway and its activation by oxidative stress. *Journal of Biological Chemistry*, 284(20), 13291–13295. <https://doi.org/10.1074/jbc.R900010200>
- Niture, S. K., Khatri, R., & Jaiswal, A. K. (2014). Regulation of Nrf2-an update. *Free Radical Biology & Medicine*, 66, 36–44. <https://doi.org/10.1016/j.freeradbiomed.2013.02.008>
- Ohkawa, H., Ohishi, N., & Yagi, K. (1979). Assay for lipid peroxides in animal tissue by thiobarbituric acid reaction. *Annals of Biochemistry*, 95, 352–358.
- Paital, B. (2014). Modulation of redox regulatory molecules and electron transport chain activity in muscle of air breathing fish *Heteropneustes fossilis* under air exposure stress. *Journal of Comparative Physiology. B, Biochemical, Systemic, and Environmental Physiology*, 184(1), 65–76. <https://doi.org/10.1007/s00360-013-0778-8>
- Paital, B., & Chainy, G. B. N. (2010). Antioxidant defenses and oxidative stress parameters in tissues of mud crab (*Scylla serrata*) with reference to changing salinity. *Comparative Biochemistry and Physiology. Toxicology & Pharmacology : CBP*, 151(1), 142–151. <https://doi.org/10.1016/j.cbpc.2009.09.007>
- Paital, B., & Chainy, G. B. N. (2012). Effects of salinity on O₂ consumption, ROS generation and oxidative stress status of gill mitochondria of the mud crab *Scylla serrata*. *Comparative Biochemistry and Physiology. Toxicology & Pharmacology : CBP*, 155(2), 228–237. <https://doi.org/10.1016/j.cbpc.2011.08.009>
- Paital, B., & Chainy, G. B. N. (2013a). Seasonal variability of antioxidant biomarkers in mud crabs (*Scylla serrata*). *Ecotoxicology and Environmental Safety*, 87, 33–41. <https://doi.org/10.1016/j.ecoenv.2012.10.006>
- Paital, B., & Chainy, G. B. N. (2013b). Modulation of expression of SOD isoenzymes in mud crab (*Scylla serrata*): effects of inhibitors, salinity and season. *Journal of Enzyme Inhibition and Medicinal Chemistry*, 28(1), 195–204. <https://doi.org/10.3109/14756366.2011.645239>
- Paital, B., & Chainy, G. B. N. (2014). Effects of temperature on complexes I and II mediated respiration, ROS generation and oxidative stress status in isolated gill mitochondria of the mud crab *Scylla serrata*. *Journal of Thermal Biology*, 41, 104–111. <https://doi.org/10.1016/j.jtherbio.2014.02.013>
- Petrulea, M. S., Duncea, I., & Muresan, A. (2009). Thyroid hormones in excess induce oxidative stress in rats. *Acta Endocrinologica (Bucharest)*, 5 (2), 155–164. <https://doi.org/10.4183/aeb.2009.155>
- Sandra, V., Schäfer, A., & Parnham, M. J. (2017). The Master Regulator of Anti-Oxidative Responses. *International Journal of Molecular Sciences*, 18(12), 2772
- Subudhi, U., Das, K., Paital, B., Bhanja, S., & Chainy, G. B. N. (2008). Alleviation of enhanced oxidative stress and oxygen consumption of L-thyroxine induced hyperthyroid rat liver mitochondria by vitamin E and curcumin. *Chemico-Biological Interactions*, 173(2), 105–114. <https://doi.org/10.1016/j.cbi.2008.02.005>
- Subudhi, U., Das, K., Paital, B., Bhanja, S., & Chainy, G. B. N. (2009). Supplementation of curcumin and vitamin E enhances oxidative stress, but restores hepatic histoarchitecture in hypothyroid rats. *Life Sciences*, 84(11-12), 372–379. <https://doi.org/10.1016/j.lfs.2008.12.024>
- Swain, S. S., Paidsetty, S. K., Dehury, B., Sahoo, J., Chaitanya, S. V., Mahapatra, N., Hussain, T., & Padhy, R. N. (2018). Molecular docking and simulation study for synthesis of alternative dapsone derivative as a newer antileprosy drug in multidrug therapy. *Journal of Cellular Biochemistry*, 119(12), 9838–9852. <https://doi.org/10.1002/jcb.27304>
- Swain, S. S., Sahu, M. C., & Padhy, R. N. (2015). In silico attempt for adduct agent(s) against malaria: Combination of chloroquine with alkaloids of *Adhatodavastica*. *Computer Methods and Programs in Biomedicine*, 122(1), 16–65. <https://doi.org/10.1016/j.cmpb.2015.06.005>
- van der Putten, H. H., Joosten, B. J., Klaren, P. H., & Everts, M. E. (2002). Uptake of tri-iodothyronine and thyroxine in myoblasts and myotubes of the embryonic heart cell line H9c2 (2-1). *Journal of Endocrinology*, 175 (3), 587–596. <https://doi.org/10.1677/joe.0.1750587>
- Vineetha, R. C., Binu, P., Arathi, P., & Nair, R. H. (2018). L-Ascorbic acid and α -Tocopherol attenuate arsenic trioxide-induced toxicity in H9c2 cardiomyocytes by the activation of Nrf2 and Bcl2 transcription factors. *Toxicology Mechanisms and Methods*, 28(5), 353–360. <https://doi.org/10.1080/15376516.2017.1422578>